scientific reports

OPEN

ERABiLNet: enhanced residual attention with bidirectional long short-term memory

Koteeswaran Seerangan[1], Malarvizhi Nandagopal[2], Resmi R. Nair[3], Sakthivel Periyasamy[4], Rutvij H. Jhaveri[5], Balamurugan Balusamy[6] & Shitharth Selvarajan[7,8]✉

Alzheimer's Disease (AD) causes slow death in brain cells due to shrinkage of brain cells which is more prevalent in older people. In most cases, the symptoms of AD are mistaken as age-related stresses. The most widely utilized method to detect AD is Magnetic Resonance Imaging (MRI). Along with Artificial Intelligence (AI) techniques, the efficacy of identifying diseases related to the brain has become easier. But, the identical phenotype makes it challenging to identify the disease from the neuro-images. Hence, a deep learning method to detect AD at the beginning stage is suggested in this work. The newly implemented "Enhanced Residual Attention with Bi-directional Long Short-Term Memory (Bi-LSTM) (ERABi-LNet)" is used in the detection phase to identify the AD from the MRI images. This model is used for enhancing the performance of the Alzheimer's detection in scale of 2–5%, minimizing the error rates, increasing the balance of the model, so that the multi-class problems are supported. At first, MRI images are given to "Residual Attention Network (RAN)", which is specially developed with three convolutional layers, namely atrous, dilated and Depth-Wise Separable (DWS), to obtain the relevant attributes. The most appropriate attributes are determined by these layers, and subjected to target-based fusion. Then the fused attributes are fed into the "Attention-based Bi-LSTM". The final outcome is obtained from this unit. The detection efficiency based on median is 26.37% and accuracy is 97.367% obtained by tuning the parameters in the ERABi-LNet with the help of Modified Search and Rescue Operations (MCDMR-SRO). The obtained results are compared with ROA-ERABi-LNet, EOO-ERABi-LNet, GTBO-ERABi-LNet and SRO-ERABi-LNet respectively. The ERABi_LNet thus provides enhanced accuracy and other performance metrics compared to such deep learning models. The proposed method has the better sensitivity, specificity, F1-Score and False Positive Rate compared with all the above mentioned competing models with values such as 97.49%.97.84%,97.74% and 2.616 respective;y. This ensures that the model has better learning capabilities and provides lesser false positives with balanced prediction.

Keywords Alzheimer's disease, Magnetic resonance imaging, Enhanced residual attention with bidirectional long short term memory, Target-based feature fusion, Modified search and rescue operations

AD is a commonly found neurological degenerative disorder. The occurrence of this disease is more common nowadays, which often develops slowly and gets worse with time. It accounts for 60–70% of dementia cases. The most prevalent initial sign is the person's troubled recall of recent events. Language difficulties, confusion, and behavioral problems can all be indicators of advanced disease. As a person's health deteriorates, they frequently isolate themselves from friends and family. Body functions gradually deteriorate, which eventually results in death. According to Alzheimer's Disease International (ADI), there are more than 50 million dementia sufferers

[1]S.A. Engineering College (Autonomous), Chennai, Tamil Nadu 600077, India. [2]Department of Computer Science and Engineering, School of Computing, Vel Tech Rangarajan Dr. Sagunthala R&D Institute of Science and Technology, Avadi, Chennai, Tamil Nadu 600062, India. [3]Department of Electronics and Communication Engineering, Saveetha Engineering College (Autonomous), Chennai, Tamil Nadu 602105, India. [4]Department of Electronics and Communication Engineering, Anna University, Chennai, Tamil Nadu 600025, India. [5]Department of Computer Science and Engineering, School of Technology, Pandit Deendayal Energy University, Gandhinagar, Gujarat, India. [6]Shiv Nadar (Institution of Eminence Deemed to Be University), Noida, Uttar Pradesh 201314, India. [7]Department of Computer Science, Kebri Dehar University, 250 Kebri Dehar, Ethiopia. [8]School of Built Environment, Engineering and Computing, Leeds Beckett University, Leeds LS6 3QS, United Kingdom. ✉email: ShitharthS@kdu.edu.et

1

globally. This number is expected to rise to 152 million by 2050, which translates to one dementia case every three seconds. By 2030, dementia is expected to cost $1 trillion annually and will likely quadruple that amount at present[1].

Alzheimer's disease in particular is one of the most expensive diseases for nations around the world. These expenses will definitely rise and constitute a significant social issue and financial burden as populations' age is higher. Direct and indirect medical expenditures are included in the costs of AD, and these costs differ between nations based on the availability of social care for AD patients. Periodical check-ups, hospital stays, medical procedures, residential nursing, and household charges are examples of direct costs. The price of informal care and the productivity loss of informal caregivers are examples of indirect costs.

The fact that there is currently no effective treatment for AD presents the biggest difficulty for experts in the field. Despite this, the available treatments for AD can reduce symptoms or halt their progression. Therefore, it is crucial to catch AD in its prodromal stage[1], in order to prevent the high care expenses associated with AD patients, which are predicted to rise sharply. Computer-Aided System (CAD) is employed for accurate and early AD detection. Traditional machine learning algorithms commonly use two types of features, namely region of interest (ROI)-based features and voxel-based features, for the early AD diagnosis, more precisely, the measurements heavily rely on the fundamental hypotheses about anatomical or functional abnormalities in the brain, including regional cortical thickness, hippocampus volume, and gray matter volume.

The presence of this disease can be recognized by the offset of certain symptoms like declined memory, behavioral changes, disturbance in thinking ability, visuospatial disturbances, and disorientation[2]. These symptoms are often mistaken for stress-related side effects. Thus, they are ignored in most cases. The early detection of AD is important because AD can eventually kill the brain cells. The diagnosis of AD is partially possible by recognizing these symptoms. But, for complete diagnosis and accurate detection, the biomarkers in the Cerebrospinal Fluid (CSF) of the brain have to be identified[3]. If not cured, AD can lead to dementia which may affect the normal functioning of humans[4]. The main reason for AD is the formation of protein which causes tangles and plaques around the brain's neurons. This leads to the expansion of the ventricles and shrinkage of the hippocampus and lobes[5]. This disease cannot be recovered, if it affects the brain completely. AD permanently disturbs the normal life of the people who are affected by it[6]. Till now, the causative agent of AD remains mysterious. Once this occurs, AD can neither be cured nor reversed. AD and normal aging behaviors are often confused by a pre-clinical phase of AD called "Mild Cognitive Impairment (MCI)"[7].

The initial diagnostic procedure that is adapted to detect AD is the MRI scan. MRI gives details about the healthiness of the human body. Since it is a non-invasive technique, it is quite popular and simple[8]. Also, MRI offers rich knowledge and efficient diagnosis of brain-related diseases. There are several improvements in CAD, because of the development of medical diagnosis procedures[9]. Deep learning techniques, along with Computer-Aided Diagnostic (CAD) systems, together proved to be an effective tool for detecting disease at its beginning stage[10]. CAD-aided MRI has shown efficient results in detecting AD in older people[11]. The other causes of dementia are ruled out by the usage Structural MRI (SMRI) technique, which has the ability to identify damages in the brain, while confirming the symptom to be caused due to AD[12].

The most commonly used detection methods for AD recognition in the past decades have been based on "machine learning approaches"[13]. Among all the machine learning techniques, "Support Vector Machine (SVM)" is the widely remarkable in disease classification. For diagnosing cancer, classifying Electroencephalogram (EEG) signals, and detecting AD, SVM is commonly used. Even for remote sensing applications, SVM is utilized[14]. The SVM functions by maximizing the boundary among two classes using a convex Quadratic Programming Problem (QPP) for the purpose of finding an ideal hyperplane. Various SVM models are designed to enhance the generalizing capability of the SVM[15]. However, the time required by the SVM to tackle the QPP makes it difficult to implement in many applications. The least-square SVM is generated to tackle the time consumption issues in SVM.

Traditional approaches rely on manual feature extraction, which is laborious, prone to human error, and significantly depends on technical expertise. Therefore, deep learning, particularly, Convolutional Neural Networks (CNNs), is a successful method to solve these issues. Additionally with increased efficiency, CNN has demonstrated significant performance in diagnosing AD and it does not require manual feature extraction because it does it automatically[1]. Deep learning-based feature mining methods have shown prominent results, since it has the capability to obtain both global and local features from the given input, offering a huge volume of features to train the neural structures[16]. Automated extraction of high-level features is possible by deep learning strategy. The most adopted deep learning techniques in medical applications are "Recurrent Neural Networks (RNN)" , variants of CNN models like GoogleNet, AlexNet, and ResNet[17]. Yet, these models are utilized only for classification purposes, because of the black-box characteristics of CNN models. Even though efficient segmentation of the neuro-images is possible by all these deep learning models, the classification outcomes provided by CNN are not up to the mark. Better features help in better learning of the deep learning models. Thus, better classification results are obtained[18]. Therefore, an efficient and automated model for detecting AD using deep learning method is deployed in this work.

The use of convolutional and recurrent neural networks (CNN-RNN), traditional biLSTM, and fully stacked (FSbiLSTM), DL-based MRI-PET imaging approaches are proposed in the work. This includes fusion of neuro-imaging features with not only genomics data but also post-mortem of the pathological correlation. The majority of current diagnoses use a single imaging modality, and the demand for multimodal imaging has arisen as a result of considerable changes in technology in the fields of structural, functional MRI, diffusion, and functional imaging[19]. Automated clinical diagnosis and prognosis have already benefited significantly from these recent discoveries, and further rapid advancements leveraging ML and DL techniques are expected.

The objectives of this detection model development are provided as follows.

- To conduct background study and enlighten literature review with existing methodologies of AD detection with respect to CAD, machine learning and deep learning techniques.
- To propose a novel method called "MSRO-ERABi-LNET" based on deep learning-aided AD detection framework with RAN model and attention-based Bi-LSTM. A RAN network is specially designed by replacing the general convolutional layer with atrous, dilated, and DWS convolutions in order to mine the attributes from the input MRI images to get the target-based fused features for efficient detection of AD. Also MSRO algorithm is used for "tuning the steps per epoch, the epoch count, and number of hidden neurons in the ERABi-LNet model" with the aim of enhancing detection performance.
- To test and validate the proposed methodology on performance metrics like algorithm evaluation, performance evaluation, convergence assessment, feature-based examination, accuracy and efficiency in AD detection.
- To compare the performance of proposed methodology with existing techniques such as ROA-ERABi-LNet, EOO-ERABi-LNet, GTBO-ERABi-LNet and SRO-ERABi-LNet respectively.

Thus the contributions of the paper can be summarized as follows,

- The proposed model of ERABi-LNet provides enhancement of the performance compared with the similar deep image neural network models with significant improvements on the performance metrics using search and rescue optimization.
- The proposed ERABi-LNet employs Alzheimer detection on the patients based on the MRI scan images acquired from the patients, where MRI images are more complex than the normal scan and other radiological images.
- This proposed method deploys search and rescue optimization which is integrated with conventional CNN networks which increases the optimization of searching the best solutions, which are features that correspond to Alzheimer detection.
- The proposed method overcomes the preprocessing overhead (CNN), size and complexity of the models (VGG) and other constraints such as error, latency etc. The search and rescue optimization enhances the model speed of convergence and performance.
- The proposed model provides better performance for a multi-class classification problem , with negligible time, space and cost constraints compared to its predecessor models

Contributions of the paper
Thus the contributions of the paper can be summarized as follows,

- The proposed model of ERABi-LNet provides enhancement of the performance compared with the similar deep image neural network models with significant improvements on the performance metrics using search and rescue optimization.
- The proposed ERABi-LNet employs Alzheimer detection on the patients based on the MRI scan images acquired from the patients, where MRI images are complex over the normal scan and other radiological images.
- This proposed method deploys search and rescue optimization which is integrated with conventional CNN networks which increases the optimization of searching the best solutions, which are features that correspond to Alzheimer detection.
- The proposed method overcomes the preprocessing overhead (CNN), size and complexity of the models (VGG) and other constraints such as error, latency etc. The search and rescue optimization enhances the model speed of convergence and performance.
- The proposed model provides better performance for a multi-class classification problem , with negligible time, space and cost constraints compared to its predecessor models

Paper organization
This paper is further organized as given below, the first part brings the motivation and contribution, of the related research. In the second part, the execution of ERABi-LNet for AD detection utilizing MRI images is presented. The third part is the development of the ERABi-LNet-based AD detection model from the MRI images. The fourth part provides the overall steps in developing the ERABi-LNet-based AD detection model, along with the description of the heuristic algorithm. The results and the discussions followed by it are given in the fifth part. The conclusion of this research work is provided in the sixth part.

Related works
In 2022, Kwon and Faisal[20] have designed a CNN model for extracting relevant biomarkers in order to classify the brain images obtained from SMRI. The data was collected from the SMRI brain images was AD Neuro-imaging Initiative (ADNI) dataset. Features from various layers were fused to obtain relevant features. The computational complexity of this model was lesser, because of the utilization of few parameters. Experimental results showed that the recommended model was efficient in diagnosing AD.

In 2022, Tanveer et al.[21] have suggested a Deep Transfer Ensemble (DTE) model to classify AD. The variations obtained by the local optimal solutions, collected from several independent models and the distinctions of the features were enhanced by the DTE by means of randomizing the model's parameters. The proposed DTE

framework's performance was better in both small and larger datasets. The accuracy offered by the suggested model in classifying AD was maximum compared with the classical AD classification frameworks.

In 2022, Muhammad et al.[22] have used a deep CNN model to classify AD from MRI images. A thermal map of the brain was obtained by this model. For a small dataset, this model precisely differentiated various beginning stages of AD. This model was built with fewer parameters and provided an inexpensive classification model. The imbalance issues in the dataset were resolved by using an oversampling approach. The performance offered by this recommended model in classifying the beginning stages of AD was better than other existing techniques.

In 2022, Sharma et al.[23] have executed an approach to detect AD at its initial stage. The deep learning model was built with a neural network. The features were extracted using the VGG-16 model. Two distinct MRI datasets with a huge volume of sample images were utilized to diagnose AD by the developed neural network. Simulation outcomes showed better diagnosing ability of the suggested neural network in diagnosing the early stage of AD.

In 2023, Geneedy et al.[17] have deployed a shallow CNN in order to accurately stratify and diagnose the various stages of AD. The T1 weighted MRI images of 2-Dimension (2D) were used as input to the pipeline model. This model provided a precise classification result, and it was faster in operation. This model was also capable of providing local and global classification results on AD. The experimental results proved the higher classification performance of the developed model compared with other existing AD classification models.

In 2023, Liu et al.[24] have utilized two tests for detecting the relevant regions of AD from the brain images. The features from these relevant regions were extracted using an unsupervised neural network. The extracted features were used to distinguish the AD data by using the clustering technique. This model was evaluated using the ADNI dataset.

In 2022, Sharma et al.[25] have suggested a deep learning-based feature mining methods. Once the features were extracted, a "Fuzzy Hyperplane Based Least Square Twin Support Vector Machine (FLS-TWSVM)" was used to classify the AD. For this purpose, they have utilized the 3D MRI image's sagittal plane slices. The ADNI dataset was adopted in this work. The hyperplane was developed by using the triangular fuzzy function in order to perform classification. The accuracy obtained by the suggested model in classifying AD was proved to be superior to the other existing models.

In 2022, Kumar et al.[26] have executed an AlexNet model for extracting the most prominent features from the input MRI images to perform an effective classification of AD. This model was able to diagnose AD at the MCI level. The "Open Access Series of Imaging Studies (OASIS) Brain" dataset was used to evaluate the developed framework by conducting experiments on a huge volume of MRI images. The suggested model recorded better accuracy when compared to the predecessors.

In 2023, Borkar et al.[27] have suggested a combination of CNN with LSTM to detect AD in its early stages, using Adam optimizer algorithm. The features of the brain were extracted from the MRI images. This method was cost-effective, with an enhanced detection accuracy of 99.7%.

In 2020, Dua et al.[28] have amalgamated Recurrent Neural Network (RNN), CNN, and LSTM for detecting AD. The variance of the three models was combined with the utilization of a bagging approach, and then the bagged model was fused with the ensemble network to determine the final detection outcomes. An accuracy of 92.22% was attained in detecting the AAD by using the suggested ensemble model.

In 2023, Ramanathan and Ramasundaram[29] have developed an automated detection model for diagnosing AD from MRI images using Discrete Wavelet Transforms (DWT) to extract essential attributes. The extracted features were reduced with the aid of the Principal Component Analysis (PCA) approach. The final detected outcome was obtained from the kernel Support Vector Machine (SVM) with a Whale Optimization Algorithm (WOA).

In 2021, Cilia et al.[30] have explored the benefits of determining the dynamic as well as the shape characteristics for efficient diagnosing of AD. The characteristics were extracted with the aid of the CNN model. The utilization of the dynamic characteristics improved the detection performance.

In 2019, Ahmed et al.[31] utilized the SoftMax cross-entropy model for classifying AD. The necessary attributes were extracted by means of an ensemble CNN model. A classification accuracy of 90.05% was attained by the recommended model.

In 2023, Chabib[32] has developed a detection model for AD using CNN with Curvelet Transform (CT) using MRI images. The gathered images were pre-processed using CT, and the detection of AD was carried out using CNN. The overall accuracy attained by the recommended model was 98.71% ± 0.05%.

In 2023, Dao et al.[33] have generated a one-dimensional CNN for classifying AD from online handwritten patterns. An efficient data augmentation approach was also determined by investing several existing augmentation methods.

In 2023, Fabietti et al.[34] have designed an Explainable Machine Learning (EXML) technique that detected AD at the early stage by utilizing the patterns from the hippocampal and cortical "Local Field Potential Signals (LFPs)". Here, the extraction of spectral, temporal, and spatial features took place, followed by the concatenation of these features. The concatenated feature was provided to the EXML for classifying AD. Around 99.4% accurate detection outcome was provided by the developed model in recognizing AD at an early stage.

In 2023, Miltiadous et al.[35] have discovered the "Dual-Input Convolution Encoder Network (DICE-net)" for classifying AD from EEG signals. The extraction of coherence, as well as band power features, took place, followed by the denoisation of the EEG signals. The classification of AD was done by the DICE-net, which was developed by utilizing Feed-forward layers, Convolution, and Transformer Encoder. The accuracy attained by the implemented model on classifying AD is 83.28%.

In 2019, Ju et al.[36] has introduced a model having the capability to detect AD at the beginning stage using a deep learning approach from Resting-state Functional MRI (R-fMRI) images. The detection was carried out using the targeted autoencoder. An enhancement of 31.21% was provided by the developed model when compared with conventional models in detecting AD.

In 2019, Afzal et al.[37] have introduced a data augmentation-aided transfer learning model for the detection AD from unbalanced 3D MRI images. The accuracy of 98.41% and 95.11% was attained on 1D and 3D views, respectively. An efficient AD stage detection was performed by the suggested model.

In 2023, Alvi et al.[38] have proposed an LSTM model for extracting deep attributes from EEG signals followed by AD classification using a sigmoid classifier for detecting AD in its beginning stage. The EEG signals were denoised and segmented, the features were extracted, and then the classification stage proceeded. A classification accuracy of 96.41% was achieved by the model.

In 2020, Jiménez-Mesa et al.[39] have suggested a machine learning model for classifying the multiclass of AD, which also addressed the issues in existing classification models. The suggested machine learning model was 67% accurate in classifying the multiclass detection of AD.

In 2023, Sekhar and Kumar[40] have developed a deep learning approach utilizing EfficientNet and UNet to detect the AD at the beginning stage.

In 2021, Raghavaiah and S. Varadarajan[41] have implemented an AD classification model by utilizing optimal Deep Neural Network (DNN). The weights in the DNN model were tuned with the aid of the Enhanced Squirrel Search Algorithm (ESSA). An enhanced outcome was obtained from the optimized deep learning-based AD detection model.

In 2022, Mahendran and Raj[42] have implemented an advanced deep learning model called the Enhanced Deep Recurrent Neural Network (EDRNN) in order to detect AD at the early stage by utilizing fused features.

In 2021, Abuhmed et al.[43] have implemented a fused model for detecting AD by utilizing multiple deep Bidirectional Long Short-Term Memory (BiLSTM) based feature extraction models. The extracted features were fed to multitask-based regression models for predicting AD in an efficient manner.

In 2020, El-Sappagh et al.[44] have suggested an ensemble model of Bi-LSTM with CNN for predicting AD from multimodal time series data. The extraction of the longitudinal features was carried out by the Bi-LSTM and CNN models separately. The extraction of the local features was done by a feed-forward neural network. These longitudinal and local features were then fused. for the efficient prediction of AD.

In 2023, Alorf and Usman[45] have introduced Graph Convolutional Network (GCN) and Stacked Sparse Autoencoder (SSA) models for classifying the multi-classes of AD from the resting-state fMRI images. Classification accuracy of 84.03 and 77.13% were achieved by the GCN and SSA models, respectively.

In 2022, Orouskhani, M. et al.[46] have proposed a deep triplet model for surface detection of Alzheimer, through MRI scan images. The model provided 99.61% of accuracy, which was comparatively better than the existing lossy triplet models.

In 2024, De Silva, K. and Kunz, H.[47] have proposed a model for prediction of Alzheimer detection, using the Convolutional Neural Network. This model provides the accuracy and PRC values of 0.89 and ROC of 0.92.

In 2024, El-Assy et al.[48] have proposed a deep learning model that reduced the CNN2 filter size of 5*5 into 3*3, along with concatenation, which increased the accuracy of these models from 95 to 99.13%.

In 2023, Pradhan et al.[49] have proposed a deep learning model for the detection of the Alzheimer. This problem is multi-classification. The method suffered from false positives, in two of the target classes out of four, such as, Mild and Moderately demented.

In 2023, Nagarathna C.R and Kusuma M.M.[50] have proposed a deep learning model for the detection of the Alzheimer . The model recorded the accuracy of 95.52% and the PRC value of 91.25%. They used CNN model for the prediction of the Alzheimer.

In 2023, Chen, Y et al.[51] have proposed an advanced approach to enhance image super-resolution reconstruction by addressing the challenge of feature information loss, inherent in deep neural network-based algorithms.

In 2024, Chen, Y et al.[52] have introduced an enhanced image inpainting network designed to overcome the challenges of information loss and structure inconsistencies commonly encountered in deep learning-based inpainting algorithms.

In 2023, Chen, Y et al.[53] have introduced a novel lightweight approach to image inpainting, focusing on optimizing restoration quality while accommodating limited processing power on various platforms.

In 2024, Chen, Y et al.[54] have proposed DNNAM model, which is a fuzzy based attention mechanism, which uses ResUNet.

This model is capable of extracting the multi-scale features, with multi-scale feature attention mechanisms.

Singh, S.et al[55] proposed a model using image transformers for detection of pneumonia disease using chest-Xrays.

Deep Neural Network (DNN) with back-propagation provided the improved visualization for the mammalian systems[56] Using DNN the connectivity between temporal lobe structures and the hippocampus, with a triplet loss, which can learn this task. With the enforcement of the factorized latent space, reconstruction of the input is done . This allows them to beat the state-of-the-art for unsupervised object segmentation on the CATER and MOVi-A,B,C benchmarks.

Diffusion Modelling (DM) for the Magnetic Resonance Imaging (MRI) RI) super-resolution (SR) reconstruction, exhibiting impressive performance, especially with regard to detailed reconstruction as per the proposed work[57]. With the high frequency and low latent space operation, the distortion-less image reconstruction was achieved.

The authors[58] implemented DeepMend model, which results with simulated fractures on synthetic and real-world scanned objects, and with scanned real fractured mugs. Compared to the existing voxel approach and two baseline methods, this work shows state-of-the-art results in accuracy and avoiding restoration artifacts over non-fracture regions of the fractured shape.

Problem statement

The detection of AD is time-consuming and computationally intensive. Classification provided by doctors is less accurate due to human intervention. In recent days, CAD has been mostly used for AD detection, but it is limited by congenital observations. Of the previous readings. AD detection approaches with their pros and cons are listed in Table 1. CNN[1] does not need pre-processing, and it requires a few of variables, thus it is not complicated. However, the classification of images is complex, and a lot of training data is required. DTE[2] has the capability to learn highly complicated patterns from the input images, and it provides high accuracy, but it is not suitable for a large number of datasets. ADD-Net[3] prevents the class imbalance problem, and it needs fewer calculation costs. Yet, it does not achieve desirable results. VGG16[4] has high computational capacity, and it is used to create image embedding vectors. However, it takes a lot of disk space and bandwidth, and it is very slow to train. CNN[5] provides both global and local classification, and it is useful in dealing with data shortages in an unbalanced dataset. But, the performance and effectiveness of the prediction process are low. Unsupervised learning[6] needs only small MRI scans, and the dimensionality reduction can be easily accomplished. FLS-TWSVM[7] eliminates the outliers, and it is highly effective in high dimensional spaces and it is also relatively memory efficient. However it requires more training time, and it does not apply to large datasets. AlexNet[8] is used to effectively extract visual patterns, and it takes less time to train. However, it cannot effectively solve the problem of gradient vanishing. Therefore, a deep learning-based AD detection using MRI is developed for the effective identification of AD.

Research gap

- The existing systems focussed mainly on accuracy whereas, the other performance metrics were not evaluated proportionately. This indicates that these works rarely worked on class imbalance and missing value imputation.
- Hyperparameter evaluation is an essential part of model evaluation, which is essential when handling the image classification.
- Most of the existing systems had issues with the size of the training data, which is essential to meet the performance requirements and to overcome class imbalance.
- For a novel proposed method, there is a huge need for the exhaustive comparison of the proposed model or algorithm with the similar working models to ensure that the proposed model or algorithm meets the requirements of the classification.

Author [citation]	Methodology	Features	Challenges
Kwon and Faisal[20]	CNN	• It does not need pre-processing • It requires a few variables, thus it is not complicated	• Classification of images is complex • A lot of training data is required
Tanveer *et al.*[21]	DTE	• It has the capability to learn highly complicated patterns from the input images • It provides high accuracy	• It is not suitable for a large number of datasets
Muhammad et al.[22]	ADD-Net	• It prevents the class imbalance problem • It needs fewer calculation costs	• It does not achieve desirable results
Sharma et al.[23]	VGG16	• It has a high computational capacity • It is used to create image embedding vectors	• It takes a lot of disk space and bandwidth • It is slow
Geneedy et al.[17]	CNN	• It provides both global and local classification • It is useful in dealing with data shortages in an unbalanced dataset	• The performance and effectiveness of the prediction process are low
Liu et al.[24]	Unsupervised learning	• It need only a few MRI scans • Dimensionality reduction can be easily accomplished	• It is computationally expensive • It provides less accuracy and does not provide precise results
Sharma et al.[25]	FLS-TWSVM	• It eliminates the outliers • It is highly effective in high dimensional spaces and also relatively memory efficient	• It requires more training time • Processing of large datasets is complicated
Kumar et al.[26]	AlexNet	• It is used to effectively extract visual patterns • It takes less time to train	• It cannot effectively solve the problem of gradient vanishing
Orouskhani, M. et al.[46]	Conditional Deep Triplet	• This model provides accuracy of around 99.61% • Short learning and deep metric model	• The stability of the model is not analyzed with PRC curves and ROC Estimation
DeSilva et al.[47]	Convolutional Neural Network	• Experimentation on MIRAD Dataset • Preprocessing with Mathew Correlation Co-efficient estimation	• PRC values are 0.89 and the ROC value is only around 0.92
El-Assy et al.[48]	Modified CNN and LSTM	• Reduced Filter Size • Concatenation with accuracy of 99.13% • Multi-Class classification on AD datasets	• Accuracy was analysed but no emphasis of PRC curve and ROC estimation. Lack of sensitivity and specific analysis
Pradhal et a.[49]	Deep Learning Techniques	• Multi class classification	• Lesser performance due to false positives on two of the classes such as Mild and Moderate Demented
Nagarathna C.R et al.[50]	Deep Learning Techniques	• Multi class classification • Multi perceptron Network, Decision Tree,SVM, Random Forest are used	• 95.52% of Accuracy and PRC vslues of 91.25%

Table 1. Features and challenges of previously existing ad classification approaches.

Materials and methods
The identification of AD at the beginning will save the life of the patient. The primary diagnosis method for detecting the AD is the usage of MRI scan images. However, the detection of the AD from these scan images would provide different results that varies with the perception of the radiologist. Also, manual detection of AD is time-consuming. So, an efficient AD detection model using deep learning techniques is generated in the paper.

Alzheimer's disease MRI image collection
The dataset for performing AD detection is obtained through online means. The MRI scan images of the patients are gathered from two benchmark websites. A detailed description of the obtained MRI image data is listed in Table 2.

The MRI images obtained from the above websites are denoted by CI_{il}^{MRI}. These images are given to the classifier to detect AD. The sample images obtained from the above sources are shown in Fig. 1.

Data preprocessing
Preprocessing of the images is done to enhance the quality of MRI images and remove artifacts that may affect analysis. The techniques performed consisted of:

- Noise Reduction: Gaussian filtering technique and motion correction is performed to reduce noise and improve image clarity.
- Intensity Normalization: This helped to provide with consistency across different MRI scans.

Then, augmentation of data is done to increase the diversity of the training dataset, improving the generalization ability of the model. The images are modified by rotation, translation, scaling and flipping. After this, feature extraction processes are applied. It involves transforming MRI images into a compact and informative representation. Texture analysis is performed which involves characterizing spatial patterns and textures within MRI images using techniques like gray-level co-occurrence matrices (GLCM) or Gabor filters to capture subtle structural abnormalities associated with Alzheimer's disease. Then, feature fusion techniques are performed. Feature fusion involves combining multiple sets of features to enhance Alzheimer's disease identification performance.

Four key metrics stand out in this evaluation process. Accuracy measures the proportion of correctly classified instances. Precision focuses on the accuracy of positive predictions, gauging the model's ability to avoid false positives. Recall, also known as sensitivity, assesses the model's capability to identify all relevant instances, particularly crucial when avoiding false negatives is paramount. Lastly, the F1 score strikes a balance between precision and recall, offering a combined measure of a model's performance.

Hyperparameter analysis

System model
RAN-based feature extraction
The attributes from the obtained MRI images CI_{il}^{MRI} from various websites are extracted using the RAN model. The arrangement of a large number of attention layers constitutes the RAN[55]. Every single attention layer has mask and trunk layers. The mask layers perform differentiable soft attention operations. Let m be the input provided to the RAN. A mask $P(m)$ that has a dimension similar to the trunk layer's features $D(m)$ is created by the mask layer. The trunk layer has residual blocks. The utilization of the differentiable soft attention mechanism helps to train the attention block more easily, and the differentiable operation helps to obtain an automated training process. The output is expressed as in Eq. (1).

$$N_{n,l,k} = P_{n,l,k} * D_{n,l,k} \tag{1}$$

In Eq. (1), the term n denotes the index of the spatial representation, which has a value $n \in \{1, ..., R * U\}$, l denotes the index of the channel, which has a value $l \in \{1, ..., V\}$, V denotes the height of the frame and U denotes the height of the frame. Top-down and bottom-up functions are carried out by the mask layer in order to alter the attributes that are obtained from the trunk layer. This acts like a feature selector as it provides weighted attributes if the trunk D is multiplied by the mask P. The differentiable capability of the mask amends the gradients while back propagation. An inbuilt noise filter is also provided in this network to eliminate the noisy label. The noise filter is given by Eq. (2).

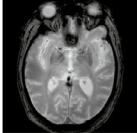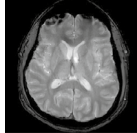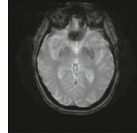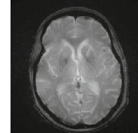| Sl. No	Name of the dataset source	Available link	Description
1)	"Alzheimers-Disease-5-Class-Dataset-ADNI"	"https://www.kaggle.com/datasets/madhucharan/alzheimersdisease5classdatasetadni access date: 2023–06-08"	Five classes of AD are provided, which includes LMCI, AD, MCI, CN, and EMCI. A total of 1296 files are given
2)	Alzheimer's Dataset (4 class of Images)	"https://www.kaggle.com/datasets/tourist55/alzheimers-dataset-4-class-of-images access date: 2023–06-08"	A file count of 6400 is available. The AD severity such as "mild, very mild, moderate, and non-demented" is provided in this dataset

Table 2. AD MRI image dataset's description.
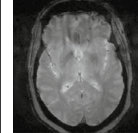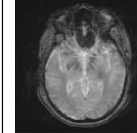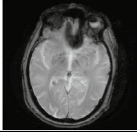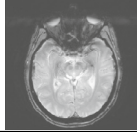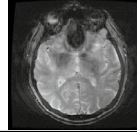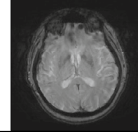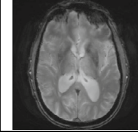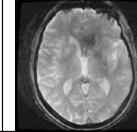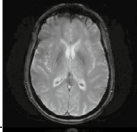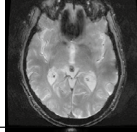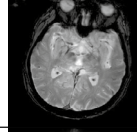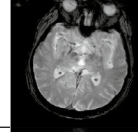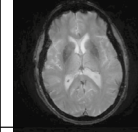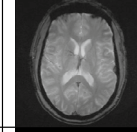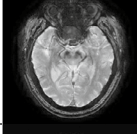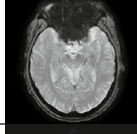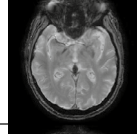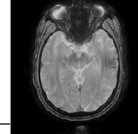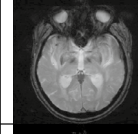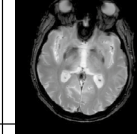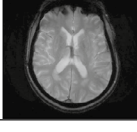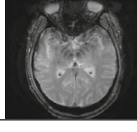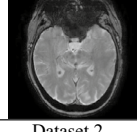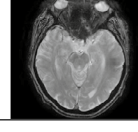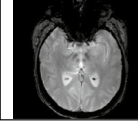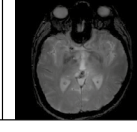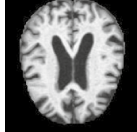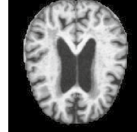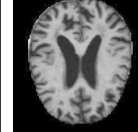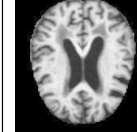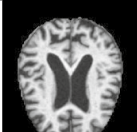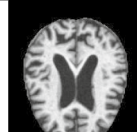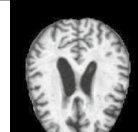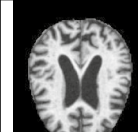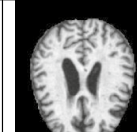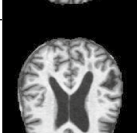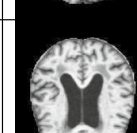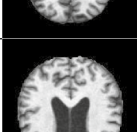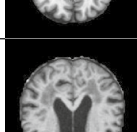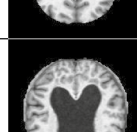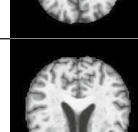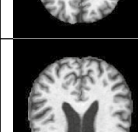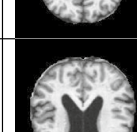
Class/ sample Image	MRI image 1	MRI image 2	MRI image 3	MRI image 4	MRI image 5	MRI image 6
Dataset 1						
AD						
CN						
EMCI						
LMCI						
MCI						
Dataset 2						
MildDemented						
ModerateDemented						
NonDemented						
VeryMildDemented						

Fig. 1. Sample images collected for developing an efficient AD detection model using deep learning technique.

$$\frac{\partial P(m, \delta_m) Q(m, \delta_m)}{\partial \delta_j} = P(m, \delta_m) \frac{\partial Q(m, \delta_m)}{\partial \delta_j} \tag{2}$$

In Eq. (2), the term δ_m indicates the parameter of the mask layer and δ_j indicatesthe trunk layer parameter. From the above Eq. (2), it is seen that the mask layer has the ability to decide whether to keep an incorrect attribute from the trunk layer or not. The most crucial attributes are obtained by utilizing the attention layers that are stacked against one another. However, the normal stacking operation degrades the performance of the RAN. Also, the major characteristics of the attributes generated from the trunk layer can be distorted by using soft attention. The $H(m)$ is approximated to the actual attributes $W(m)$, which is due to the function of residual attention learning. The $P(m)$ is in the range $[0, 1]$. The main function of the mask layer is to improve performance and reduce the noises in the trunk layer. The progressive nature of stacked attention layers provides a space

for residual attention learning. The soft mask can be bypassed using this residual attention learning. This also helps to preserve the better qualities in the actual function. Residual attention learning enhances the network's performance by improving the depth of the network. The bottom-up operation of the mask layer helps to gather the global details, and the top-down operation fuses the actual function map with the gathered global details. Max pooling operation takes place multiple times once the input is provided. After multiple residual blocks, the linear interpolation will sample the outputs. The output's length is maintained as similar to that of the input map by keeping the bilinear interpolation as same as the number of pooling functions. To use the RAN model for extract the attributes from the input MRI images, the general architecture of the RAN is slightly modified. The single 1×1 convolutional layers in the conventional RAN model are replaced by an atrous convolutional layer, dilated convolutional layer, and DWS convolutional layers. These layers help to obtain distinct features from the MRI images.

Target-based feature fusion

The general convolutional layers in the RAN are modified with Artous, dilated and DWS convolutional layers. These layers are used to mine the attributes from the obtained MRI images CI_{il}^{MRI}. The atrous convolutional layer helps to obtain rich inputs attribute maps. The dilated convolutional layer helps to extract the intrinsically sequential details from the input image without any additional parameter requirement. The DWS convolutional layer obtains accurate attributes from the MRI images without increasing the parameters of the model. The obtained features from these three convolutional layers of the RAN model, namely atrous, dilated, and DWS convolutional layers, are fused together to get the target-based fused features TF_{xk}^{RAN}. The pictorial illustration of the modified RAN architecture for performing target-based feature fusion is shown in Fig. 2.

Developed ERABi-LNet-based AD Identification

The MRI images CI_{il}^{MRI} are provided to the ERABi-LNet model for detecting AD. The ERABi-LNet model is developed by combining a specially developed RAN structure with attention-based Bi-LSTM. The convolutional layers in the traditional RAN are upgraded with atrous, dilated and DWS convolutional layers. From these three layers, the attributes from the MRI images are extracted. The mined attributes are concatenated. The "target-based
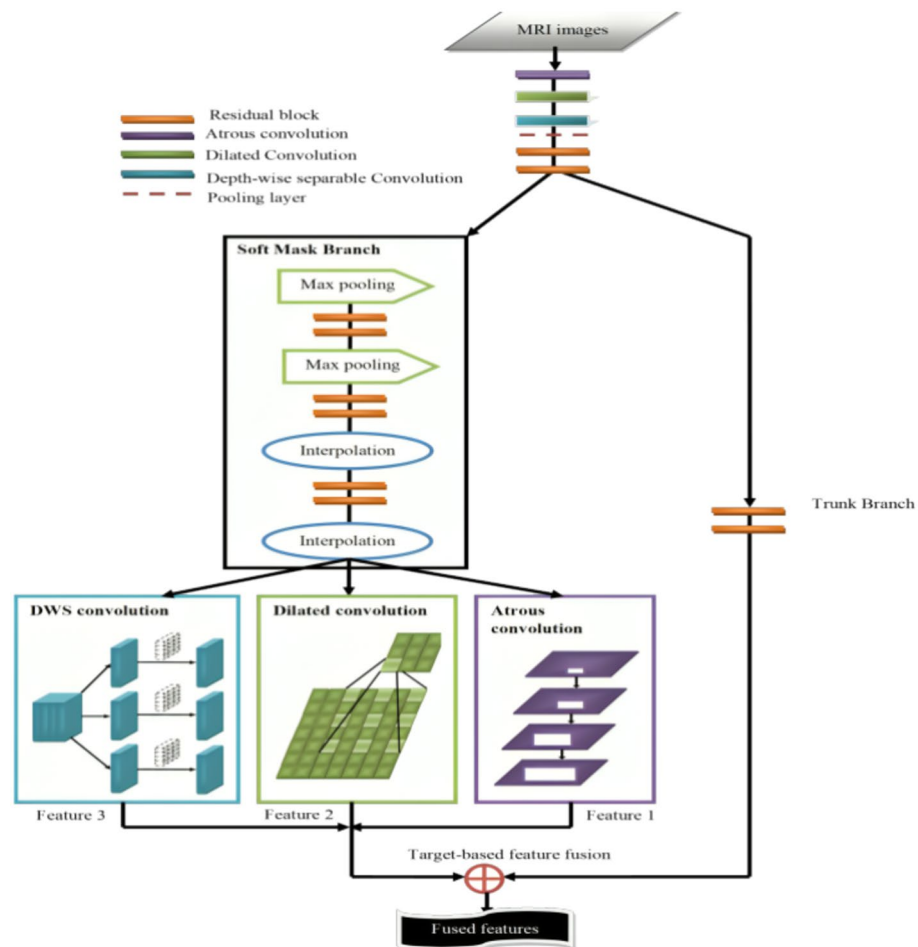
Fig. 2. Graphical illustration of the modified RAN system for target-based feature fusion.

fused attributes" TF_{xk}^{RAN} are now given to the "attention-based Bi-LSTM" model. The attention-based Bi-LSTM is generated by combining the Bi-LSTM with an "attention layer". The Bi-LSTM[44] is a network that has both backward and forward LSTM structures. The Bi-LSTM is used because of its ability to learn, bi-directional context relationships and long-term dependencies. It also helps to resolve issues with exploding and disappearing gradients. Inputs in both backward and forward directions are provided to the Bi-LSTM. Both the inputs to the backward and forward layers are linked to a single layer of output. Each LSTM in the Bi-LSTM structure consists of "output, input, and forget gates". These three gates are responsible for the updation and preservation of the LSTM's cell state. The cell state is determined by the input gate, which is given by Eq. (3).

$$m_p = \sigma \left(X_m * \left[v_{p-1}, Z_p' \right] + Y_m \right) \tag{3}$$

The prior cell state's information is preserved by the forget gate, which is given by Eq. (4).

$$s_p = \sigma \left(X_s * \left[v_{p-1}, Z_p' \right] + Y_s \right) \tag{4}$$

The output from the ceil state is regulated by the output gate which is provided by Eq. (5).

$$q_p = \sigma \left(X_q * \left[v_{p-1}, Z_p' \right] + Y_q \right) \tag{5}$$

The term σ in Eq. (3), Eq. (4), and Eq. (4) denotes the sigmoid trigger function. The current cell state is provided by Eq. (6).

$$M_p = s_p * M_{p-1} + m_p * \tanh \left(X_M * \left[v_{p-1}, Z_p' \right] + Y_M \right) \tag{6}$$

In Eq. (3), Eq. (4), Eq. (5), and Eq. (6), the terms X_m, X_s, X_q and X_M denotes the weight matrix, the terms Y_m, Y_s, Y_q and Y_M denotes the bias vector, and the term v_p denotes the hidden state of the LSTM which is given by Eq. (7).

$$v_p = q_p * \tanh \left(M_p \right) \tag{7}$$

The term p in Eq. (3), Eq. (4), Eq. (5), Eq. (6), and Eq. (7) denotes the time. Using all these gates, the information is stored in the LSTM unit of the Bi-LSTM. The backward and the forward LSTM units are connected in parallel. Both LSTMs operate as a conventional LSTM network but in opposite directions. These two opposite-directional LSTM units aid the Bi-LSTM in preserving both future and past information. The input m_p at an instant p is handled by both the forward and the backward LSTMs. The hidden state representation of the Bi-LSTM is given by Eq. (8).

$$v_p = u_f \vec{v}_p + u_b \overleftarrow{v}_p + Y \tag{8}$$

The term u_f in Eq. (8) indicates the weight of the forward LSTM, $\vec{v}_p$ indicates the forward LSTM's output, Y indicates the bias, u_b denotes the weight of the backward LSTM, and $\overleftarrow{v}_p$ denotes the output obtained from the backward LSTM. The unnecessary information from the images is discredited by means of the attention[28]. Thus, the identification accuracy of the Bi-LSTM model can be increased using the attention mechanism. Scores are provided for every feature based on their significance.

$$w_m^p = X_w \tanh \left(X_s C_m + X_v C_{v-1} + Y_w \right) \tag{9}$$

The term Y_w in Eq. (9) indicates the bias, and the term $v-1$ indicates "prior hidden state", and the terms X_w, X_s and X_v denote the weight vectors that are utilized for training. The attention is determined by Eq. (10).

$$\mu_m^p = \frac{e^{\left(\mu_m^p \right)}}{\sum\limits_{m=1}^{z} e^{\left(\mu_m^p \right)}} \tag{10}$$

The weighted summation of the attributes of the images is computed using Eq. (11).

$$C_p' = \sum_{m=1}^{z} \mu_m^p C_m \tag{11}$$

The final detection outcomes are obtained from the attention-based Bi-LSTM network. The detection accuracy and precision are enhanced by tuning the variables like "the steps per epoch, the hidden neuron count and the number of epochs of the ERABi-LSTM model" using the MSRO algorithm. The major objective of optimizing these parameters improve the detection precision, NPV and accuracy and to reduce the FPR. This objective is mathematically given by Eq. (12).

$$OJ = \underset{\left\{ es_{ab}^{ERAB}, he_{cd}^{ERAB}, se_{ef}^{ERAN} \right\}}{\arg \min} \left(\frac{1}{AB + BC + CD} + DE \right) \tag{12}$$

The term *AB* in Eq. (12) denotes the accuracy, *BC* denotes the precision, *CD* denotes the "Negative Predictive Value (NPV)", *DE* denotes the "False Positive Rate (FPR)", es_{ab}^{ERAB} denotes the tuned count of epochs in the range [5, 50], he_{cd}^{ERAB} indicates the "tuned number of hidden neurons" in the range [5, 255], and se_{ef}^{ERAB} denotes the tuned steps per epochs which are in the range [50, 250]. The "NPV" is calculated as in Eq. (13).

$$CD = \frac{AX}{AX + BZ} \tag{13}$$

In Eq. (13), the term *BZ* denotes the "false negatives" and *AX* denotes the "true negatives". The "precision" computes as in Eq. (14).

$$BC = \frac{AZ}{AZ + BX} \tag{14}$$

In Eq. (14), the term *BX* denotes the "false positives" and *AZ* denotes the "true positives". The "accuracy" is evaluated as in Eq. (15).

$$AB = \frac{AX + AZ}{AX + BX + AZ + BZ} \tag{15}$$

The "False Positive Rate (FPR)" is computed using Eq. (16).

$$DE = \frac{BX}{AX + BX} \tag{16}$$

The illustration of the ERABi-LNet-based AD detection model is given in Fig. 3.

Overall Steps of Developed ERABi-LNet-based AD Identification Model with the Description of Heuristic Algorithm
Overall Steps of Developed ERABi-LNet
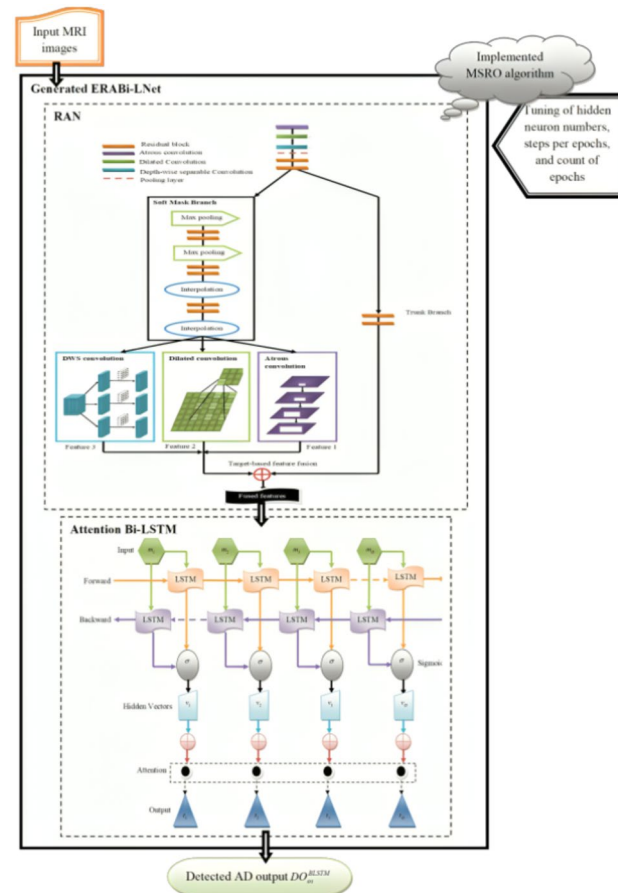The overall steps that take place in the developed ERABi-LNet model for AD detection are given as follows.

Fig. 3. Illustration of ERABi-LSTM-based AD detection model.

1) At first, the MRI images are fed to the "RAN model".

2) The "RAN model" is developed such that the general convolutional layers of the RAN are replaced by atrous, dilated and DWS convolutional layers.

3) Three sets of features are obtained separately from the atrous, dilated and DWS convolutional layers of RAN.

4) The extracted features are then fused together.

5) The fused features are given to the "attention-based Bi-LSTM model".

6) The classification outcome is generated by the attention-based Bi-LSTM model.

Architecture and working

The MRI images are obtained from various benchmark data sources for generating an efficient AD identification framework. The gathered MRI images are fed to the executed ERABi-LNet model. In the ERABi-LNet model, there are two distinct systems provided. The first one is a RAN, and the second one is the attention-based Bi-LSTM. The RAN is specially implemented such that it is provided with three types of convolutional layers. The general convolutional layer is the RAN is replaced with atrous, dilated and DWS convolutional layers that are arranged back to one another. These convolutional layers help to get the appropriate features from the input MRI images. The relevant and the appropriate features are extracted by using atrous, dilated and DWS convolutional layers of the RAN. The obtained features are then used to perform a target-based fusion of features. The target-based fused features obtained from the RAN are now given to the "attention-based Bi-LSTM" framework. From the attention-Bi-LSTM, the final detection outcome of AD is determined. The efficiency of the AD detection and the result accuracy is improved by tuning the variables, such as the "steps per epoch, hidden neurons, and epochs" of the ERABi-LNet model using the MSRO algorithm. The result from the developed ERABi-LNet-based AD detection framework is compared with other existing AD detection models to evaluate the efficient operation of the deployed ERABi-Lnet model in detecting AD. The pictorial illustration of the deployed deep learning-based AD detection model is depicted in Fig. 4.

Proposed MSRO algorithm.

Modified Search and Rescue Optimization (MSRO) is a metaheuristic algorithm that takes inspiration from the organized efforts of search and rescue teams in emergency situations. It is a variant of the traditional Search and Rescue Optimization (SRO) algorithm but incorporates modifications aimed at enhancing its performance and efficiency. In MSRO, candidate solutions are represented as a set of search agents, analogous to search and rescue teams. Each search agent corresponds to a potential solution to the optimization problem being addressed. These solutions are evaluated based on their fitness, which represents how well they satisfy the objectives of the problem. MSRO algorithm is used for tuning the variables in the ERABi-LNet-based AD detection model, which includes "the number of epochs, the hidden neuron count and the steps per epochs". These parameters are optimized to enhance the accuracy, NPV, and precision of AD detection while reducing the FPR. Because of the better performance and the ability to avoid local optimum, the SRO algorithm is selected in this work. The random parameter e_4 in the traditional SROA is modified using a fitness-based concept in the suggested MSRO algorithm to maintain the exploitation and the exploration effectively. The updation of the random number is carried out as given in Eq. (17).

$$e_4 = \frac{wstft * mnft}{bstft} \tag{17}$$

In Eq. (17), the term *wstft* indicates the "worst fitness value",*mnft* denotes the "mean fitness value", and *bstft* denotes the "best fitness value". The value of e_4 in conventional SROA is within the range $[0, 1]$ which is modified by using the above Eq. (25) in the MSRO algorithm. MSRO strikes a balance between local exploitation and global exploration. It utilizes local search mechanisms to exploit promising regions of the solution space, refining the solutions and improving their quality. At the same time, it incorporates mechanisms for global exploration to prevent premature convergence to suboptimal solutions. The search process in MSRO continues until certain termination criteria are met. These criteria include reaching a maximum number of iterations, achieving a satisfactory level of solution quality, or exceeding a predefined computational budget. In the MSRO algorithm, methods are employed to systematically explore solution spaces, evaluate fitness, and balance between local exploitation and global exploration. Initially, a population of search agents representing potential solutions is initialized across the solution space. These agents undergo fitness evaluation based on an objective function, guiding their movements through the solution space. Local search mechanisms refine solutions within promising regions, while global exploration ensures diversity and prevents premature convergence. Adaptation and evolution mechanisms allow search agents to dynamically adjust positions, responding to changes in the solution landscape. Through iterative improvement and parameter tuning, MSRO navigates optimization landscapes effectively, converging towards high-quality solutions.

The applications of the MSRO algorithm span across various domains, offering versatile solutions to complex optimization challenges. In engineering, MSRO finds utility in tasks such as optimizing design parameters, scheduling production processes, and enhancing resource allocation. Logistics and supply chain management benefit from MSRO's ability to optimize routing, inventory management, and distribution strategies. In finance, MSRO aids in portfolio optimization, risk management, and algorithmic trading strategies. Telecommunications benefit from MSRO's optimization of network design, spectrum allocation, and signal processing algorithms. Additionally, MSRO proves valuable in healthcare for tasks such as optimizing treatment plans, resource allocation in hospitals, and predictive modeling for disease diagnosis and prognosis. Its adaptability, efficiency,
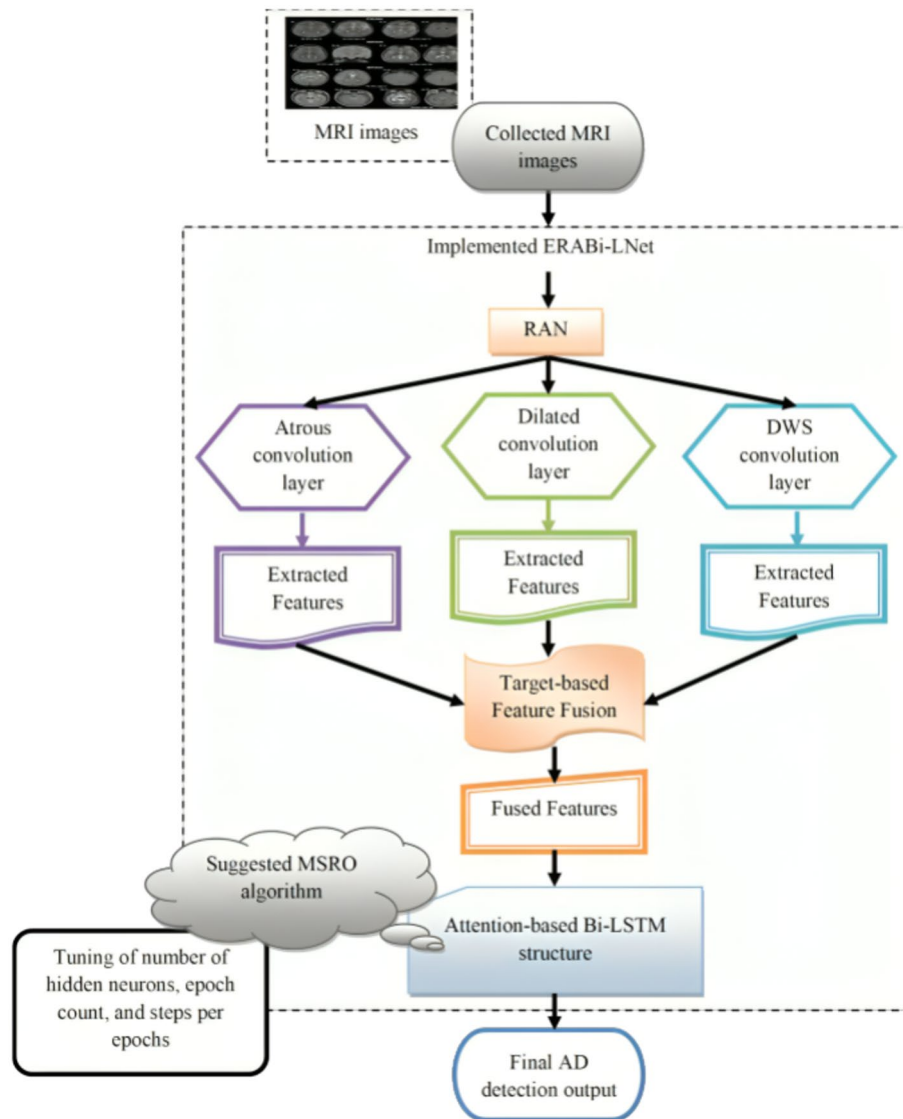
Fig. 4. Pictorial Illustration of the Proposed Deep Learning-based AD Detection Framework.

and effectiveness make MSRO a powerful tool for addressing diverse optimization problems across industries, facilitating enhanced decision-making and resource utilization.

SROA
The process of locating an individual who is in distress is called searching. The process of providing aid to the individual who is in distress and making them feel safer is called rescue. These two processes serve as the backbone of the SROA[45]. The maximization problems are solved by using SROA. The location in which the individuals are present represents the optimization problem's solution count. The clues that are present in these locations indicate the fitness of the respective solutions. The members of the rescue team collect clues during the entire search process. The existing clues are left behind whenever a new clue is obtained. However, the details on the left clue is retained by the team members. The locations in which the unwanted clues are left are stored in A. The locations of the team members are saved in B. The location of all the clues that are found while searching for the lost individual is stored in G. The clue matrix G is constituted based on B and A. Based on the clue matrix G, the generation of the new solution in individual and social searching phases takes place. Both the memory matrix A and the position matrix B has the same dimension. These two matrices are of order $E \times F$ in which the count of the team members is represented by F, and the problem's dimension is represented by E. At every searching phase, the values of the memory matrix A, position matrix B, and clue matrix G are amended. The clue matrix is provided in Eq. (18).

$$G = \begin{bmatrix} B \\ A \end{bmatrix} = \begin{bmatrix} B_{11} & \cdots & B_{1F} \\ \vdots & \ddots & \vdots \\ B_{E1} & \cdots & B_{EF} \\ A_{11} & \cdots & A_{1F} \\ \vdots & \ddots & \vdots \\ A_{E1} & \cdots & A_{EF} \end{bmatrix} \tag{18}$$

The term A_{1F} in Eq. (18) denotes the 1st memory's location at the Fth dimension and B_{E1} denotes the Eth individual's location at the 1st dimension. The individual and the team searching phases are obtained as given below.

Team searching. The locations from which the clues are obtained are used to figure out the lost person in the team searching phase. At first, a clue is selected arbitrarily from all the obtained clues. The direction in which the search takes place is given by Eq. (19).

$$H_a = (B_a - G_c); \; c \neq a \tag{19}$$

The term H_a in Eq. (19) denotes the ath individual's direction of searching, B_a denotes the ath individual's location, and G_c denotes the cth clue's location. The term c represents a random variable that ranges from $[1, 2E]$. Since no particular area is searched repeatedly, the movement of the individuals in the team towards other individuals in the team is restricted in RSOA. Therefore, not every dimension of B_a are altered on the basis of Eq. (18). A binomial crossover function is utilized to perform this function. When the newly obtained clue is better than the old one, then the region surrounding the obtained new clue and around H_a is searched. Else, the region surrounding the present location is searched. The team searching phase is represented by Eq. (20).

$$B_{a,b}^* = \begin{cases} B_{a,b} & e_2 \geq I \\ \begin{cases} B_{a,b} + e_1 \times (B_{a,b} - G_{c,b}) & d(G_c) \leq d(B_a) \\ G_{c,b} + e_1 \times (B_{a,b} - G_{c,b}) & d(G_c) > d(B_a) \end{cases} & e_2 < I \end{cases} \tag{20}$$

In Eq. (19), the term $G_{c,b}$ indicates the cth clue's location at b^{th} dimension, $d(B_a)$ denotes the fitness B_a, $B_{a,b}^*$ indicates the ath individual's upgraded location at b^{th} dimension, e_2 denotes a variable uniformly distributed arbitrary variable which varies from $[0, 1]$, $d(G_c)$ indicates the fitness of G_c, e_1 denotes a constant uniformly distributed arbitrary number within the limit $[-1, 1]$, and I denotes the parameter of the SROA within the limit $[0, 1]$. When $e_2 < I$, the value of $b = b_r$ in which b_r denotes an arbitrary variable in the range $[1, F]$. These arbitrary variables make sure that at least any one dimension of $B_{a,b}^*$ and $B_{a,b}$ are different.

Individual searching. The clues obtained from the team searching phase are utilized by the individuals to search around their present location in this individual searching section. Each B_a dimension varies. The updated position of the ath individual is given by Eq. (21).

$$B_a^* = B_a + e_3 \times (G_c - G_g); \; c \neq a \neq g \tag{21}$$

In Eq. (21), the term e_3 denotes a variable uniformly distributed arbitrary variable which varies from $[0, 1]$, and g denotes a random variable that ranges from $[1, 2E]$. Whenever an individual's location reaches the lookup area's boundary, then the location of the individual is amended using Eq. (22).

$$B_{a,b}^* = \begin{cases} \frac{B_b^{mn} + B_{a,b}}{2} & B_{a,b}^* < B_b^{mn} \\ \frac{B_b^{mx} + B_{a,b}}{2} & B_{a,b}^* > B_b^{mx} \end{cases} \tag{22}$$

The term B_b^{mn} in Eq. (22) indicates the minimum boundary of the bth dimension and B_b^{mx} denotes the maximum boundary of the bth dimension. The two searching phases takes place in every iteration of SROA. At the end of every phase, the fitness is checked with the prior fitness value. If $d(B_a)$ is less than $d(B_a^*)$, then the prior location is saved in any random location of A. The process of storage of the location in the memory matrix A is given by Eq. (23).

$$A_h = \begin{cases} A_h & d(B_a^*) \leq d(B_a) \\ B_a & d(B_a^*) > d(B_a) \end{cases} \tag{23}$$

The term h in Eq. (23) indicates an arbitrary number of ranges from $[1, E]$ and A_h denotes the hth saved clue's location. Equation (22) is taken as the updated location with the help of Eq. (24).

$$B_a = \begin{cases} B_a & d(B_a^*) \leq d(B_a) \\ B_a^* & d(B_a^*) > d(B_a) \end{cases} \tag{24}$$

Time is an important constraint that has to be considered while performing search and rescue. The largest lookup region has to be covered within a short duration of time. When no good clues are obtained from the present location of the individual, then the individual will move towards a new location in search of clues. A parameter known as an "Unsuccessful Search Number (USN)" is set as 0 for every individual if a better clue is

obtained in either of the team or individual searching phase. If no better clue is obtained, then the value of USN is increased by 1. The method of determining the value of USN is given by Eq. (25).

$$K_a = \begin{cases} 0 & d\left(B_a^*\right) \geq d(B_a) \\ K_a + 1 & d\left(B_a^*\right) < d(B_a) \end{cases} \tag{25}$$

The term K_a in Eq. (25) denotes the count of unsuccessful attempts of an individual in obtaining a better clue. If $K > J$ is satisfied, then the individual will move toward a random location in search of a better clue. The term J indicates the maximum value of USN. The individual's location in the random lookup area is given by Eq. (26).

$$B_{a,b} = B_b^{mn} + e_4 \times \left(B_b^{mx} - B_b^{mn}\right) \tag{26}$$

In Eq. (26), the term e_4 denotes a variable uniformly distributed arbitrary variable which varies from $[0, 1]$. The value of e_4 in Eq. (26) is modified using the fitness-based concept provided in Eq. (16). Both terms J and I are important control parameters in RSOA. The value of J is in the range $[0, 2 \times L_{mx}]$ in which L_{mx} denotes the maximum iteration count and $2 \times L_{mx}$ denotes the maximum searches that are carried out by every individual. The value of I is set to be 0.05, and the value of J is set to be $F \times 70$. The pseudocode of the MSRO algorithm is given in algorithm 2.

Start
 Input: $2E$ (arbitrarily populated)

Let N → Solutions in Descending Order

Target: B_{Best}- Best of the Population
Let $B \rightarrow Location\ Matrix$
Let $(P \rightarrow Population)$
Let A→ $Memory$
 Let P/2 → B
Let 1- P/2→ A

Determine I and J Parameters of the current solution

Set $K_a = 0$ denotes no unsuccessful attempts
While (true)
    For $a = (1 \rightarrow E)$
        Find Term T,
        Determine H
        For $b = (1 \rightarrow F)$
        Execute Eq. (19) and Eq. (21)
        End

        Determine A_h, B_a and K_a 2→ A_h is the memory matrix
        Search for the Ba → Random lookup for the best solution.

        Determine B_a^*
        For $b = (1 \rightarrow F)$
        Execute Eq. (21)
        End

        Determine A_h, B_a and K_a

        If $K_a > J$ then minimum qualification criteria
            For $b = (1 \rightarrow F)$

                fit | e_4 |→ fittest arbitrary variable
        Determine $B_{a,b}$ → the best solution

                End
                $K_a = 0$
            End
        End
        Determine the present best location and amend B_{Best}
    End
    Return B_{Best}
End

The flowchart for the implemented MSRO algorithm is shown in Fig. 5.

Experimentation, results and discussion

The proposed model used the MSRO algorithm for feature and location optimization. This algorithm finds the best solutions that are the features based on the "average", "worst" and "best" fitness values. The arbitrary fitness variable "e4"is estimated based on these fitness values. This is estimated as a product of worst and average fitness to the best fitness value. The fitness evaluation is done between [0 and 1] where the absolute value of e4 is checked for the optimal fitness value. Thus the feature approximation increases the accuracy and efficiency of the proposed model by reducing the false positives in the trained data. This results in the increase of the performance by 2–6% and efficiency of the existing ERABi-LNet model.

The executed AD detection framework was simulated using the "Python paradigm". The simulation was carried out with a "population number" of 10, iteration numbers of 50 and a "chromosome length" of 3. The simulated outcome from the deployed ERABi-LNet model was compared with the results obtained from the conventional classifiers like LSTM[59], "Recurrent Neural Network (RNN)"[60], Residual Network (ResNet)[61], and (Without Optimization)[62], and existing algorithms like Rider Optimization Algorithm (ROA)- ERABi-LNet[26],
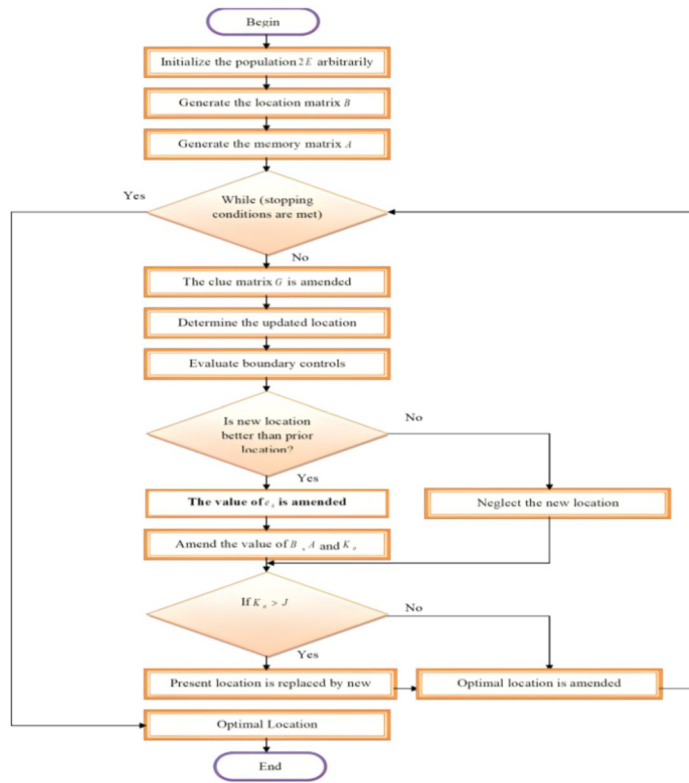
Fig. 5. Flowchart of the Executed MSRO algorithm.

Eurasian Oystercatcher Optimizer (EOO)- ERABi-LNet[60], Golden Tortoise Beetle Optimizer (GTBO)-ERABi-LNet[59], SRO-ERABi-LNet[63], respectively, in order to prove the efficiency of the generated ERABi-LNet model in detecting AD.

Evaluation measures used to assess the deployed AD detection framework

The evaluation measures used to access the deployed AD detection framework are listed as follows.

(a) The Matthews Correlation Coefficient (MCC) is computed utilizing Eq. (27).

$$EF = \frac{AX^{\star}AZ - BX^{\star}BZ}{\sqrt{(AZ + BX)(AZ + BZ)(AX + BX)(AX + BZ)}} \tag{27}$$

(b) The "F1-score" is computed with the aid of Eq. (28).

$$FG = \frac{2 * AZ}{2 * (AZ + BX + BZ)} \tag{28}$$

(c) The False Negative Rate (FNR) is determined using Eq. (29).

$$GH = \frac{BZ}{AZ + BZ} \tag{29}$$

(d) The sensitivity is computed with the help of Eq. (30).

$$HI = \frac{AZ}{AZ + BZ} \tag{30}$$

(e) The "False Discovery Rate (FDR)" is determined using Eq. (31).

$$IJ = \frac{BX}{AZ + BX} \tag{31}$$

(f) The specificity is evaluated with the aid of Eq. (32).

$$JK = \frac{AX}{AX + BX} \tag{32}$$

Performance metrices

Algorithmic evaluation of the performance of the suggested AD detection system
The algorithmic evaluation of the performance of the suggested AD detection system is shown in Fig. 6 and Fig. 7 for both Dataset 1 and Dataset 2, respectively. By analyzing dataset 1, it is found that the FPR of the recommended ERABi-LNet-based AD detection framework is 34.78%, 50%, 59.46%, and 57.14% lesser than the SRO-ERABi-LNet, GBTO-ERABi-LNet, EOO-ERABi-LNet, and ROA-ERABi-LNet, at a learning percentage of 65%.

Assessment of the performance of the executed AD detection model with traditional classifiers
The assessment of the performance of the executed AD identification system with traditional classifiers is given in Fig. 8 and Fig. 9 for the two datasets accordingly. The evaluation of the figure suggests that the precision offered by the implemented ERABi-LNet-based AD detection model is 2.17, 4.44, 6.82, and 9.3% superior to the ERABi-LNET without optimization, ResNet, RNN, and LSTM classifiers, respectively, at a learning percentage of 45 for dataset 1.

ROC Analysis on the executed AD detection framework
The ROC analysis on the executed AD detection system is given in Fig. 10. The figure shows that the "True Positive Rate (TPR)" value of the executed ERABi-LNet-based AD detection framework is 22.06%, 7.79%, 2.47%, and 1.22% more than the existing AD detection models like "LSTM, RNN, ResNet, and ERABi-LNet without optimization", respectively at an FPR value of 0.2 for dataset 2.

Features-based validation on the performance of the suggested AD detection model with other classifiers
The features-based validation on the performance of the suggested AD detection model with other classifiers regarding Dataset 1 and Dataset 2 are provided in Fig. 11 and Fig. 12. The precision of the suggested ERABi-LNet-based AD detection model is 2.13, 3.23, 4.35, and 5.5% higher than the ERABi-LNet, ResNet, RNN, and LSTM, respectively for fused features in case of dataset 2.

Features-based examination on developed AD detection framework with existing algorithms
The features-based examination of the performance of the developed AD detection framework with existing algorithms regarding Dataset 1 and Dataset 2 are given in Fig. 13 and Fig. 14. The accuracy of the developed ERABi-LNet-based AD detection model is 6.15%, 5%, 2.99%, and 1.68% more than the ROA-ERABi-LNet,
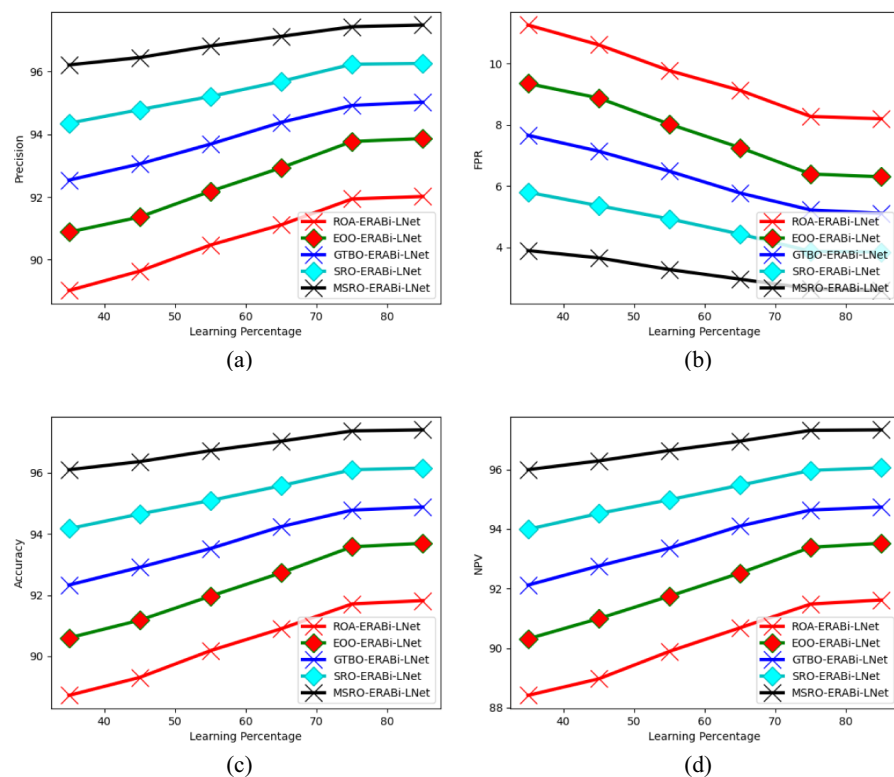

Fig. 6. Dataset 1-based Algorithmic Evaluation on the Performance of the Recommended AD Detection Framework with respect to "(**a**) Precision, (**b**) FPR (**c**) Accuracy, and (**d**) NPV.
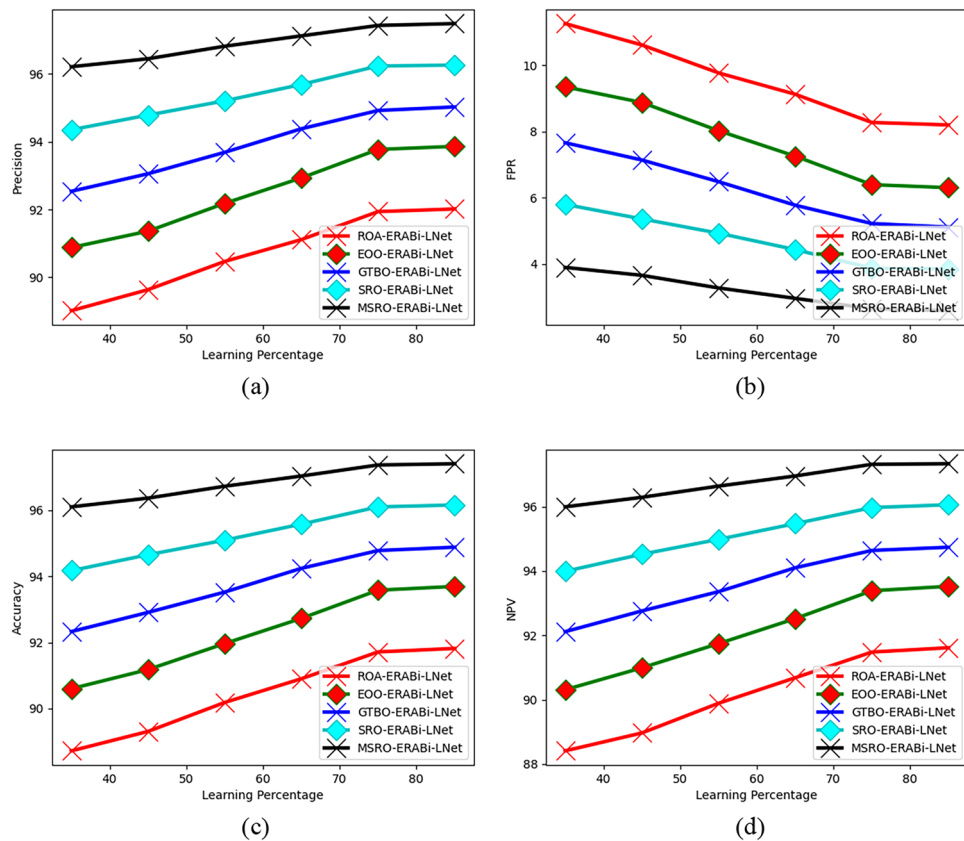
Fig. 7. Dataset 2-based Algorithmic Evaluation on the Performance of the Recommended AD Detection Framework with respect to to "(**a**) Precision, (**b**) FPR (**c**) Accuracy, and (**d**) NPV".

EOO-ERABi-LNet, GBTO-ERABi-LNet, and SRO-ERABi-LNet algorithms, respectively for dilated features for dataset 2.

Performance validation on proposed AD detection model with conventional classifiers
The performance validation of the proposed AD detection model with conventional classifiers is listed in Table 3. By validating .(Table 4)it is seen that the accuracy of the proposed ERABi-LNet framework is 6.25, 4.75, 3.42, and 2.02% higher than the LSTM, RNN, ResNet, and ERABi-LNetmodels, respectively, for dataset 1. This ensures the higher efficiency of the proposed ERABi-LNet framework in detecting AD.

Algorithmic comparison on deployed AD detection framework
The algorithmic comparison of the deployed AD detection framework is provided in Table 5. The evaluation carried out on the performance of the deployed ERABi-LNet framework with other algorithms shows that the NPV offered by the suggested ERABi-LNet model is 6.22%, 4.02%, 2.65%, and 1.37% increased than the ROA-ERABi-LNet, EOO-ERABi-LNet, GBTO-ERABi-LNet, and SRO-ERABi-LNet algorithms, respectively, for dataset 1.

Convergence assessment on suggested AD detection model
The convergence assessment of the suggested AD detection model is shown in Fig. 15 for both datasets. The cost requirement of the suggested ERABi-LNet-based AD detection model is 20, 27.27, 33.33, and 38.46% lesser than the conventional algorithms like SRO-ERABi-LNet, GBTO-ERABi-LNet, EOO-ERABi-LNet, and ROA-ERABi-LNet algorithms, respectively, for Dataset 1 at an iteration count of 20. Thus, the enhanced convergence rate suggested is proved by this assessment.

Statistical report of the implemented AD detection model
The statistical report of the deployed AD detection model is provided in Table 6. The median value of the executed ERABi-LNet-based AD detection model is 26.37%, 17.26%, 7.55%, and 5.97% decreased than the other existing algorithms, such as ROAERABi-LNet, EOO-ERABi-LNet, GBTO-ERABi-LNet, and SRO-ERABi-LNet, for dataset 1.
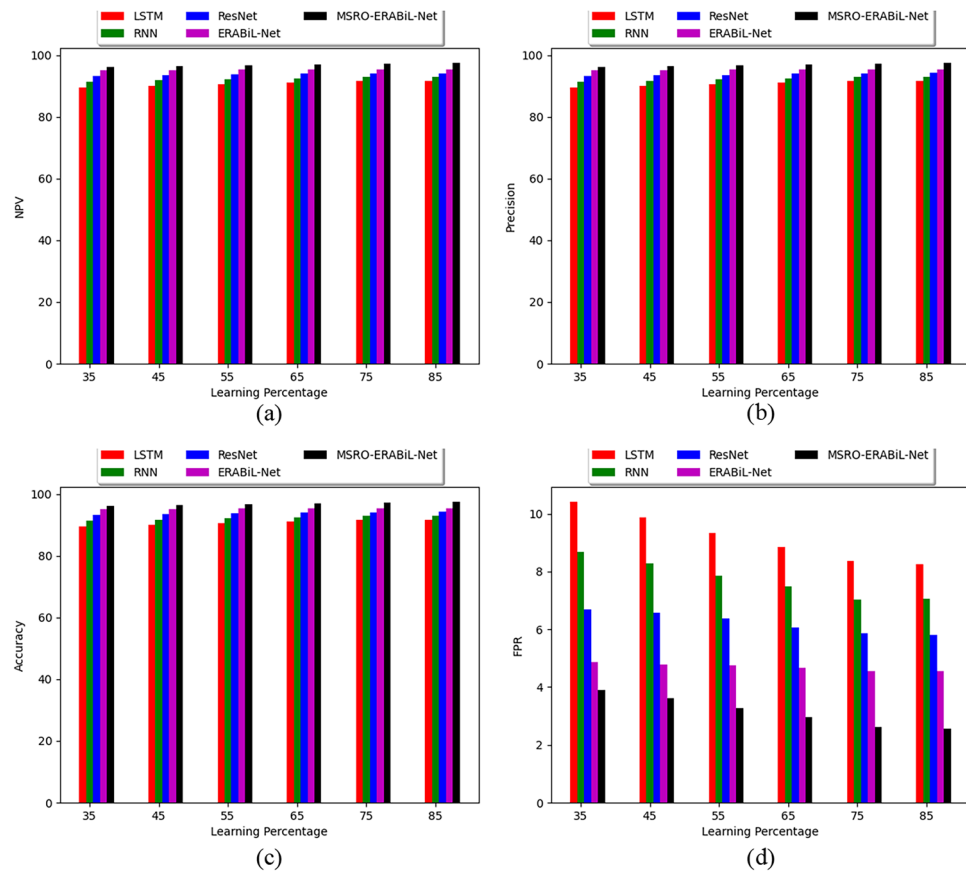
Fig. 8. Dataset 1-based Assessment of the Performance on the Implemented AD Detection Model with Traditional Classifiers in terms of "(**a**) NPV, (**b**) Precision, (**c**) Accuracy, and (**d**) FPR.

Confusion matrix examination of the executed AD detection model

The confusion matrix analysis of the executed AD detection model for "Dataset 1 and Dataset 2" is shown in Fig. 16. While analyzing the confusion matrix, which is obtained by plotting the FPR against True Positive Rate, it is seen that with decreasing TPR and FPR, the "accuracy" of the executed AD detection model is increased. The enhanced accuracy provided by this ERABi-LNet-based AD detection model is proved by analyzing the confusion matrix.

Discussion

The results of the proposed work are compared with the existing systems in order to understand the importance of the proposed method. The work presented by authors[64] indicates that voxel training with 3D CNN under transfer learning provided the best possible accuracy for AD. The proposed work presented 90.62% accuracy for ResNet-50, 93.52% accuracy for the ResNet-102 and 96.88% of accuracy for the ResNet-18 model. The proposed work outperformed the accuracy of this work by 1%. The work presented by[65] used Alzheimer Detection nework with SMOTEOMEK, where both the oversampling and undersampling are applied. This proposed work even after class balancing by over and undersampling provided the accuracy of 97.05%, which is even slightly lesser when compared with the proposed results.

A new deep networks-based AD detection system called MSRO-ERABi-LNET in which the RAN layer is replaced by atrous convolution, dilated convolution and DWS convolution. These convolutional layers helped in mining the attributes from the input MRI images. The application of the image data mining is done in the MRI images. The attention based Bi-LSTM structure has the approximated target based concatenations . The ERABi_LNet provides enhanced accuracy and other performance metrics with the better sensitivity, specificity, F1-Score and False Positive Rate compared with all the above mentioned competing models with values such as 97.49%0.97.84%,97.74% and 2.616 respectively. This ensures that the model has better learning capabilities and provides lesser false positives with balanced prediction.

These enhancements improved the efficiency of the model training and deployment. The experimental outcomes showed that the model paramaters such as accuracy, precision, recall, f1 score, false positive rate and false negative rate pf the ERABi-LNet model was 2–6% more than the LSTM, RNN, ResNet, and ERABi-LNet models. This clearly shows that the addition of the three convolution layers as transformation layers and the attention seeking Bi-LSTM structure at the input has successfully enhanced the overall performance of the model , when compared with the predecessors.The various challenges were imposed on the proposed model such as,
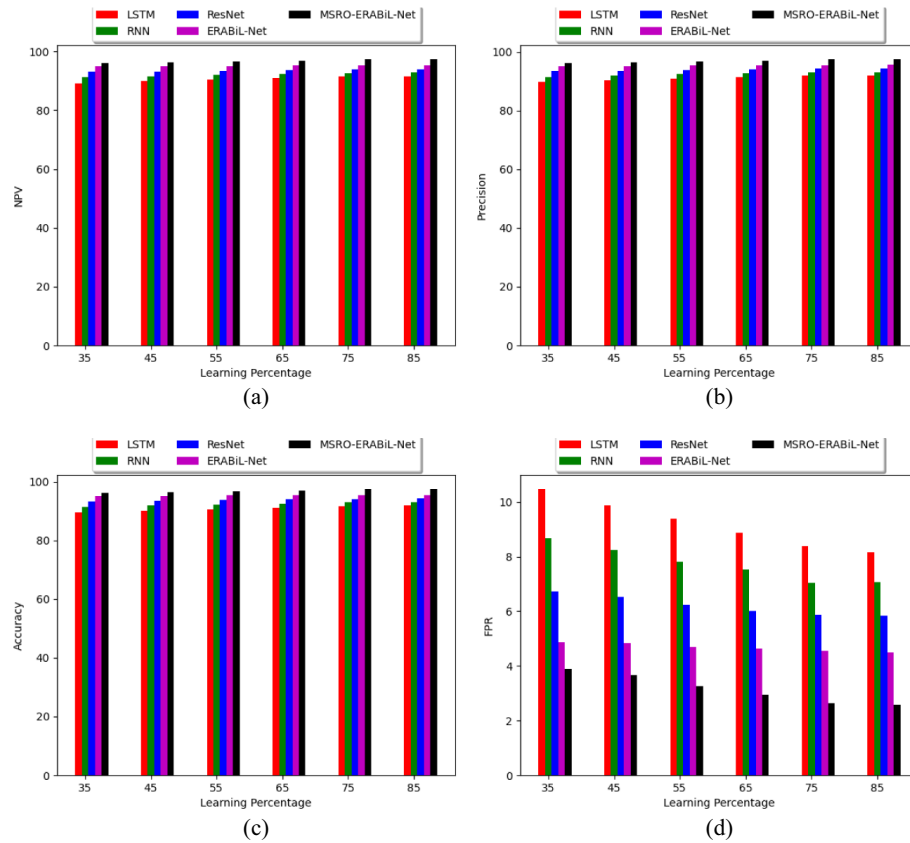
Fig. 9. Dataset 2-based Assessment of the Performance on the Implemented AD Detection Model with Traditional Classifiers in terms of "(**a**) NPV, (**b**) Precision, (**c**) Accuracy, and (**d**) FPR".
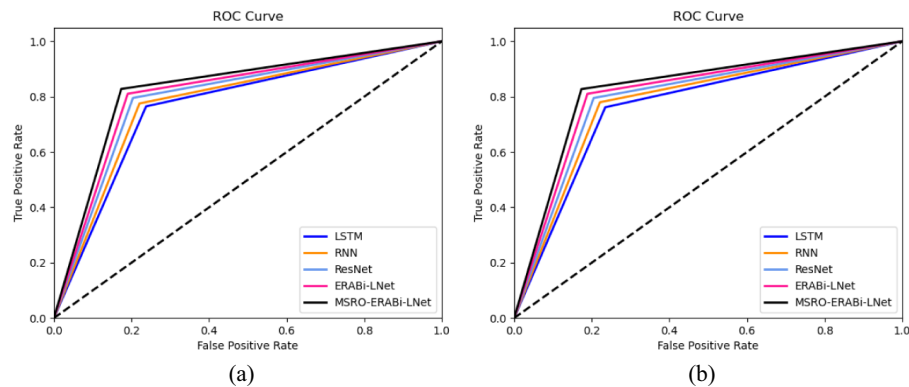
Fig. 10. ROC Analysis on the Executed AD Detection Framework regarding "(**a**) Dataset 1, and (**b**) Dataset 2".

Challenges

- The model needs to concatenate the input which increases the complexity of the model with the integration of the model especially the integration of the RAN with Bi-LSTM for attention seeking at the input side.
- The increase of the convolution layers also increases the training time reducing the speed of the model[66].
- Trade-off between the accuracy, efficiency and precision is the real challenge in the detection of AD. The complexity of the architecture definitely would compromise any one of the above requirements[67].
- This model requires high computing infrastructure, enhanced memory for data processing and the model development time is also more than the predecessors[68].
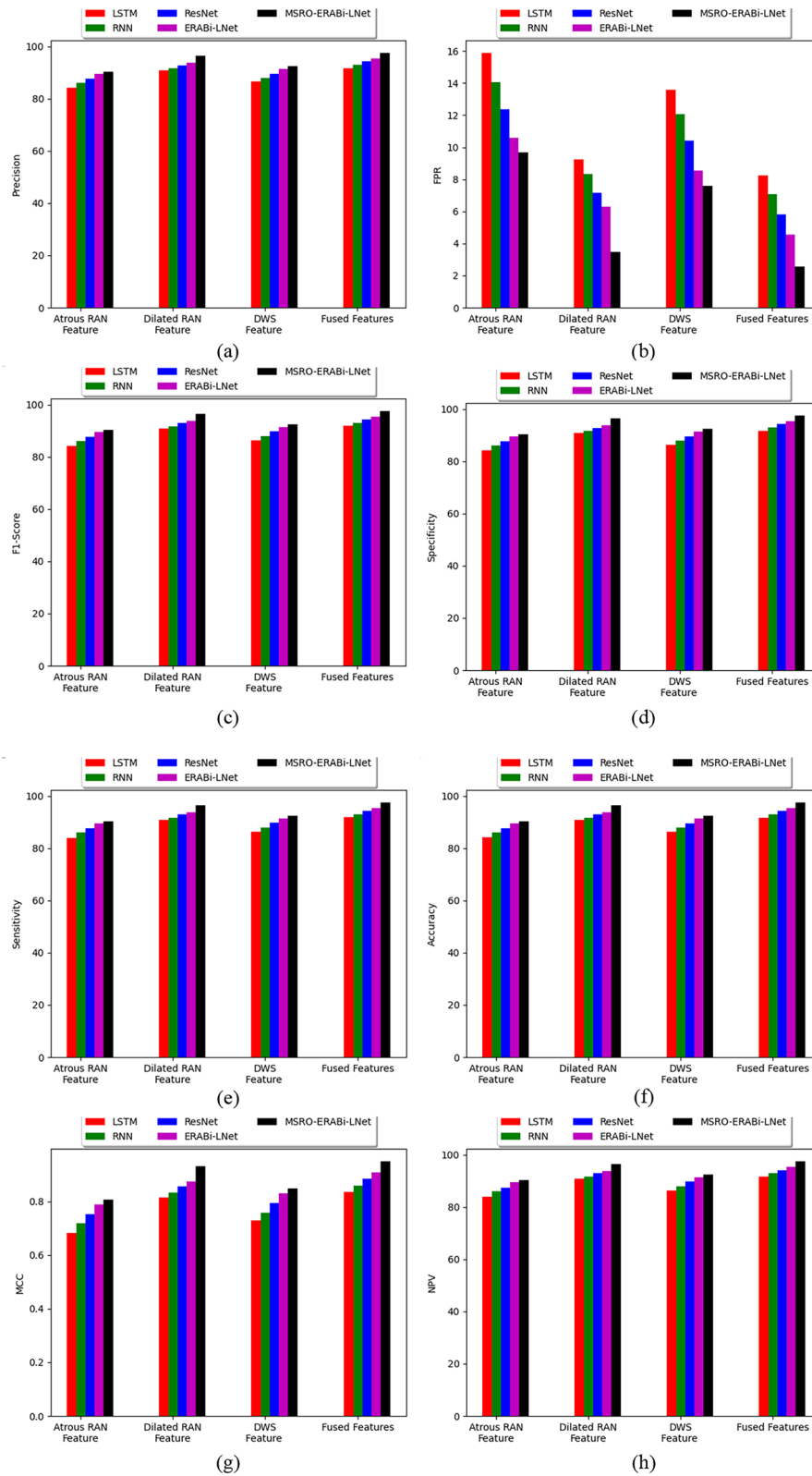
Fig. 11. Dataset 1-based Performance Validation of the Suggested AD Detection Model-based on the Extracted Features when compared against Other Classifiers with respect to "(**a**) Precision, (**b**) FPR, (**c**) F1-score, (**d**) Specificity, (**e**) Sensitivity, (**f**) Accuracy, (**g**) MCC, (**h**) NPV, (**i**) FDR, and (**j**) FNR".

Fig. 11. (continued)

- Multi- class classification generally challenged by false positives around one class, which develops a bias in the model that affects the performance of model development and the prediction[69].
- Experimental analysis of the proposed system is not conclusive, because the model is never tested and deployed on various image and pattern recognition data. The proposed model needs to be applied in various implementation scenarios to really understand the merits of the same.

Outcomes of the research

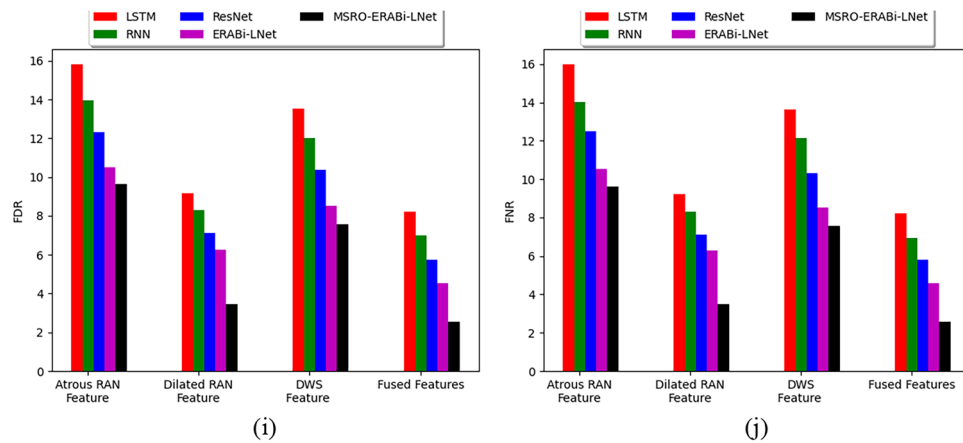- Inspite of the slow convolution and processing the model provided elevated performance with 2–6% increase on the relevant metrics.
- The statistical evaluation of the proposed model is also measured as comparatively better than the other models such as LSTM, RNN, ResNet, and ERABi-LNet models.
- Batch Size, Epochs and other hyperparameters are tuned to provide optimal performance of the model with a suitable learning rate also.
- The same model can be used for various images datasets such as EEG, Brain MRI imaging etc., which proves the adaptability and flexibility of the model design
- Training and validation errors are minimized in MSRO method to provide optimum performance and error handling capabilities.
- The proposed work provides the balanced predictability across various classes, which is really an impressive feature for a multi-class classification problem.
- The proposed work may be utilized for treating the patients with Unmanned Arial Vehicle (UAV)[70,71] and multi-path sensing networks[72,73] can be useful for patient diagnosis[74] and treatment.
- The proposed work may also be applied for sustainable application such as water quality analysis and evaluation[75] with interpretable design solutions.

Conclusion

A new deep networks-based AD detection system called MSRO-ERABi-LNET was proposed. At first, the MRI images were given to the RAN structure in which the general convolutional layer was replaced by atrous convolution, dilated convolution and DWS convolution. These convolutional layers helped in mining the attributes from the input MRI images. The extracted attributes were fused together to obtain the target-based attribute concatenations. These target-based attribute concatenations were given as input to the attention Bi-LSTM structure. The parameters in the ERABi-LNet were optimized using the newly implemented MCDMR-SRO algorithm. The identified AD was obtained from the attention-Bi-LSTM model. Various simulations proved the efficacy of the proposed ERABi-LNet framework. The experimental outcomes showed that the accuracy offered by the ERABi-LNet model was 6.25, 4.75, 3.42, and 2.02% more than the LSTM, RNN, ResNet, and ERABi-LNet models. Thus, the implemented system proved to be effective, accurate, efficient, and precise in detecting AD at the beginning stage itself. However, it was noted that the incorporation of RAN in the Bi-LSTM structure has added extra weights and parameters to the detection model. This results in the requirement of more training time for developing this model for AD detection. The requirement of resources and the memory space for processing the provided data is also more in this method. All these drawbacks will be overcome by developing an even more efficient deep learning approach in the future. Also, instead of utilizing the MRI image alone, a multi-modal detection model for detecting AD and accurately classifying it from any input, such as EEG images, handwritten patterns, and so on, will be implemented in the future. The limitations of the proposed work along with the future enhancements are listed below.
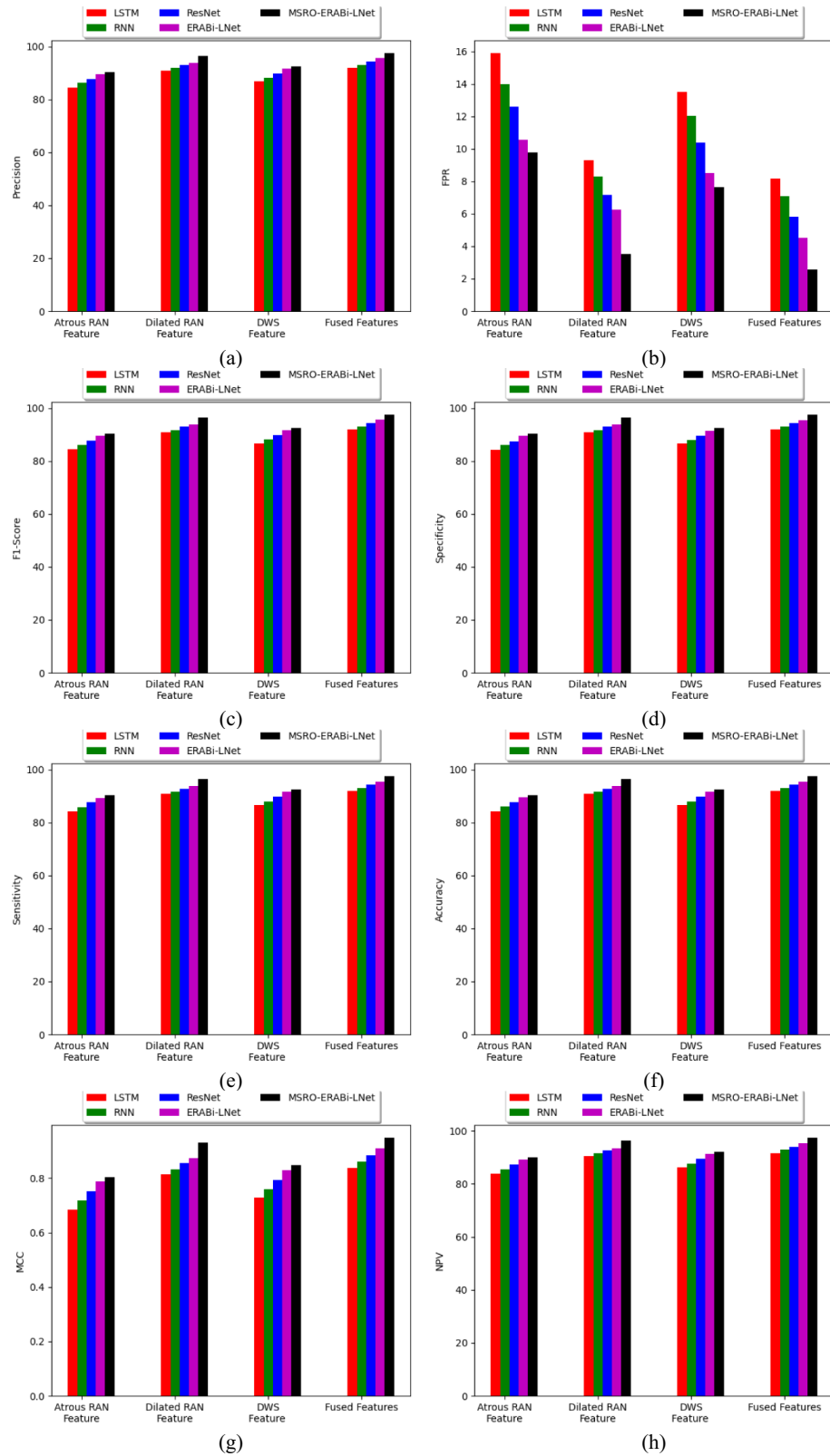
Fig. 12. Dataset 2-based Performance Validation of the Suggested AD Detection Model-based on the Extracted Features when compared against Other Classifiers with respect to "(**a**) Precision, (**b**) FPR, (**c**) F1-score, (**d**) Specificity, (**e**) Sensitivity, (**f**) Accuracy, (**g**) MCC, (**h**) NPV, (**i**) FDR, and (**j**) FNR".
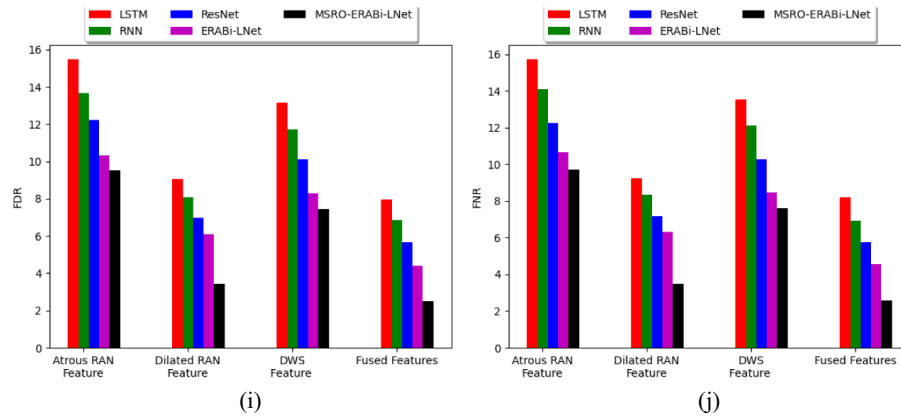
Fig. 12. (continued)

- The performance of the AD detection is evaluated on the moderately sized dataset, whereas the similar performance on large datasets would be more challenging, if there are increased false positive present in the data.
- The trade-off between the accuracy and efficiency would also be greatly challenged, in case if we have class imbalance and also introduce dropout layers, that could certainly reduce the efficiency.
- In case of multi-class classification false positives could further affect the accuracy of the model.
- The impact of the feature engineering could not be felt on datasets that acquire fewer number of features.

The proposed work can be enhanced with the following perspectives in the future implementations such as,

- The model has only been deployed on the publicly available datasets, which are not certain in determining the actual potentiality of the model in real life scenarios. Hence the model must be evaluated under the real-life datasets, with human intervention.
- The model provided better accuracy than the predecessors, but still measured with false positives in some of the classes, which needs to be addressed by enhancement of performance with hyperparameter evaluations.
- Large scale pattern analysis and recognition can be incorporated with GAN assisted neural networks for the exploration of the unknown patterns of Alzheimer's disease. The usage of autoencoders and discriminators provide diversity on the disease and the pattern analysis.
- Large language models can also be used for the prediction with search optimization with text based tokens acquired from the medical report of the patients for the comprehensive prediction of the Alzheimer's disease.

Fig. 13. Dataset 1-based Performance examination of the developed AD Detection Framework with Existing Algorithms in terms of "(**a**) NPV, (**b**) Precision, (**c**) MCC, (**d**) F1-score, (**e**) Accuracy, (**f**) FNR, (**g**) Sensitivity, (**h**) FDR, (**i**) Specificity, and (**j**) FPR".
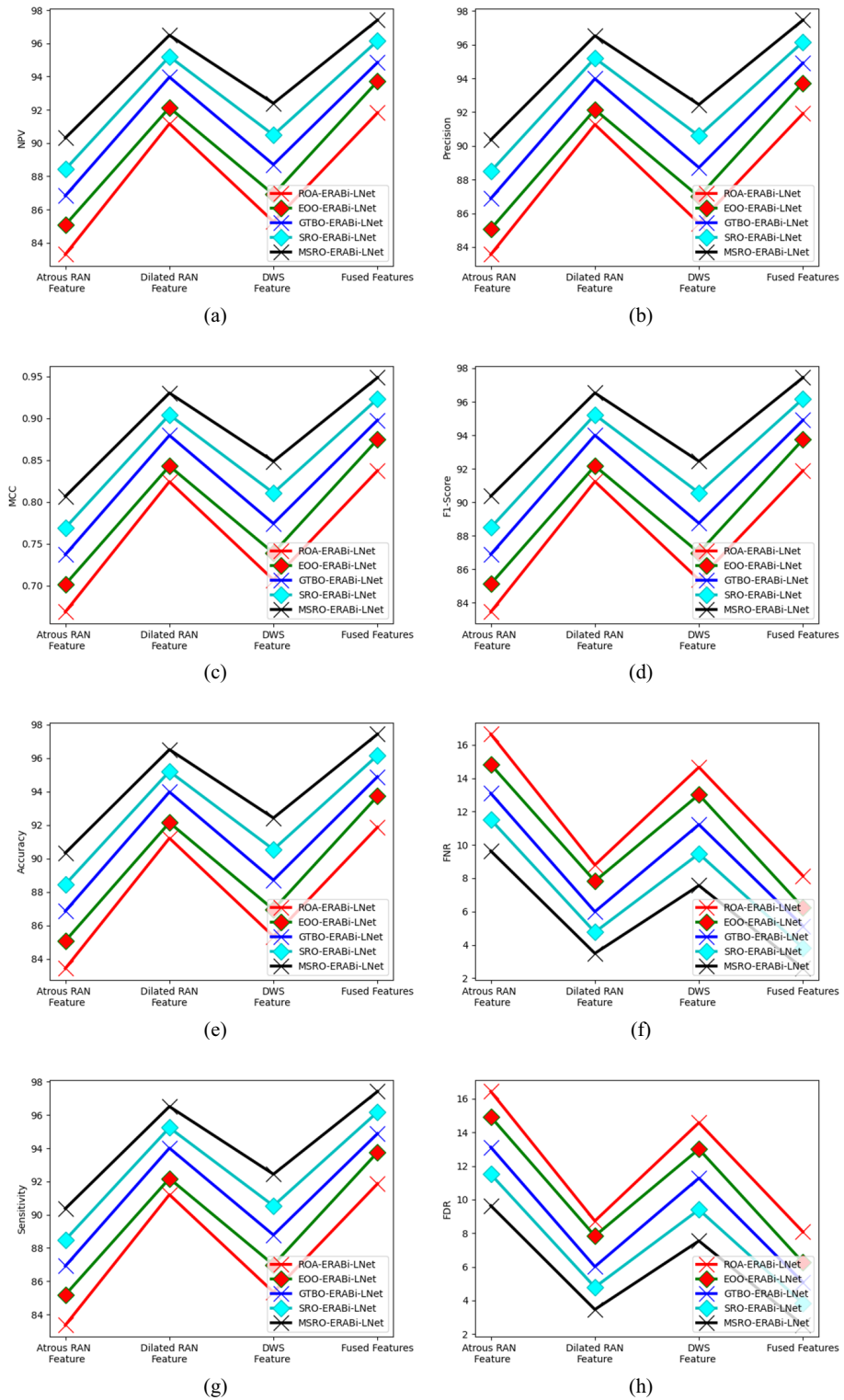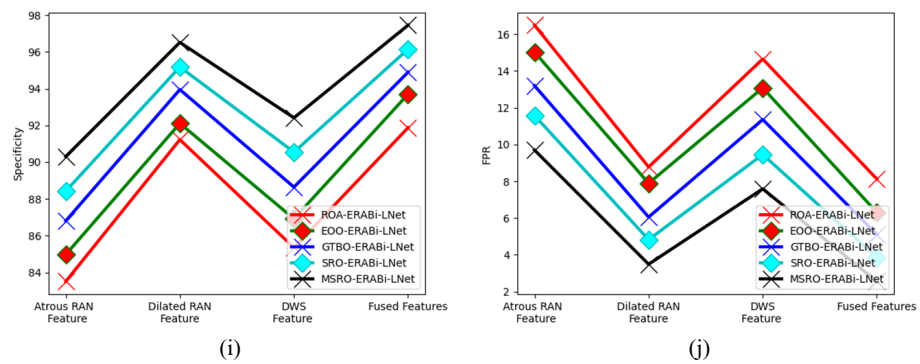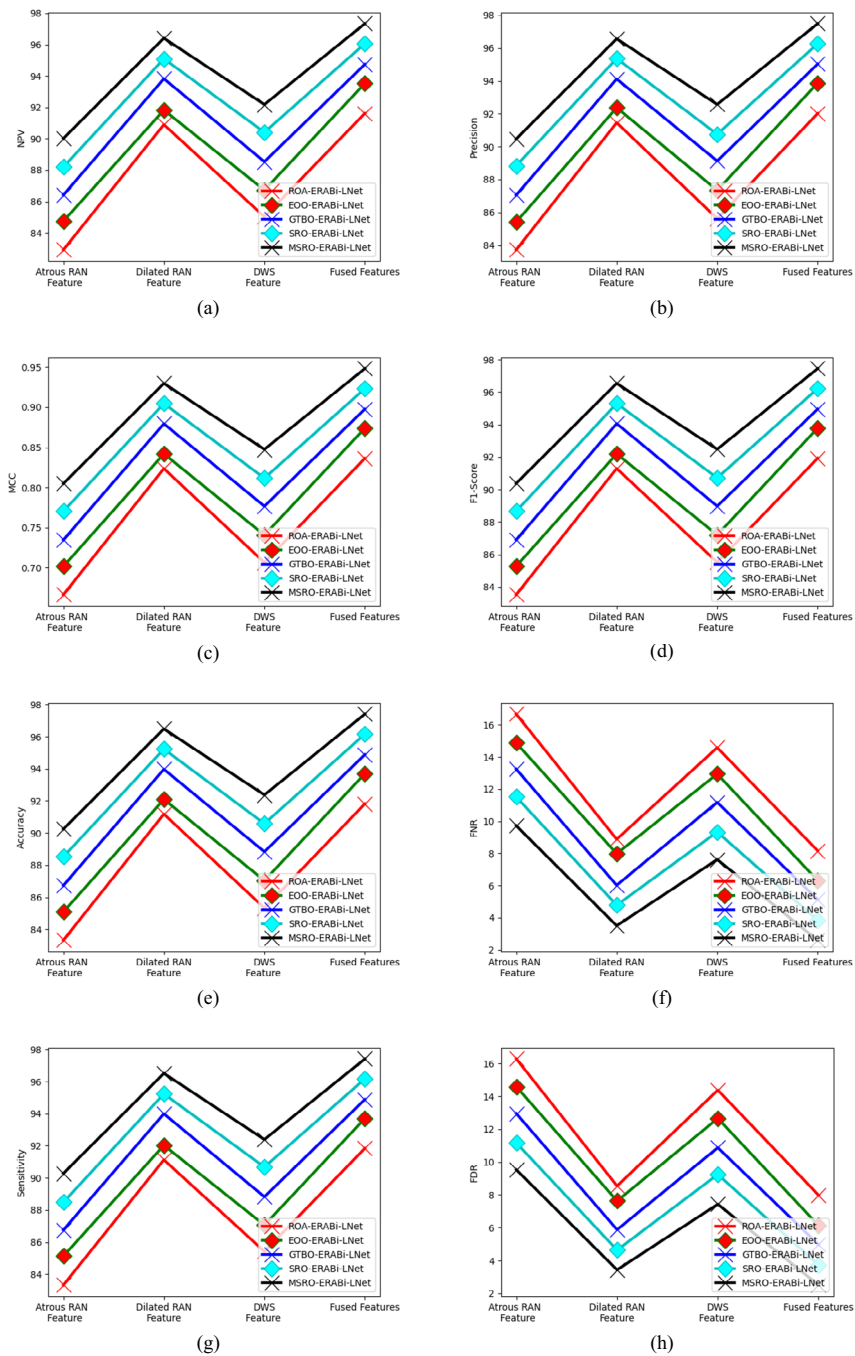
Fig. 13. (continued)

Fig. 14. Dataset 2-based Performance examination of the developed AD Detection Framework with Existing Algorithms in terms of "(**a**) NPV, (**b**) Precision, (**c**) MCC, (**d**) F1-score, (**e**) Accuracy, (**f**) FNR, (**g**) Sensitivity, (**h**) FDR, (**i**) Specificity, and (**j**) FPR".

Fig. 14. (continued)

Table 3. Performance Validation Of The Proposed Ad Detection Model With Conventional Classifiers.
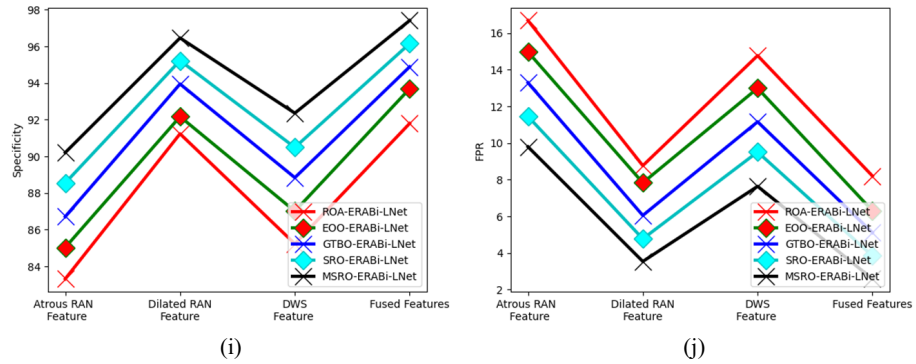
Metrics/ Classifiers	LSTM[32]	RNN[33]	ResNet[34]	ERABi-LNet[35]	MSRO-ERABi-LNET
Dataset 1					
NPV	91.603	92.901	94.118	95.405	97.335
Precision	91.672	92.999	94.182	95.470	97.398
MCC	0.833	0.859	0.883	0.909	0.947
F1-Score	91.661	92.968	94.166	95.450	97.374
Accuracy	91.638	92.950	94.150	95.438	97.367
FNR	8.351	7.063	5.850	4.570	2.651
Sensitivity	91.649	92.937	94.150	95.430	97.349
FDR	8.328	7.001	5.818	4.530	2.602
Specificity	91.626	92.963	94.150	95.445	97.384
FPR	8.374	7.037	5.850	4.555	2.616
Dataset 2					
NPV	91.549	92.714	94.002	95.294	97.317
Precision	91.851	93.150	94.280	95.560	97.432
MCC	0.834	0.859	0.883	0.909	0.947
F1-Score	91.818	93.027	94.223	95.491	97.413
Accuracy	91.702	92.935	94.143	95.429	97.376
FNR	8.215	7.097	5.834	4.578	2.607
Sensitivity	91.785	92.903	94.166	95.422	97.393
FDR	8.149	6.850	5.720	4.440	2.568
Specificity	91.617	92.967	94.119	95.436	97.358
FPR	8.383	7.033	5.881	4.564	2.642

Table 4. Hyper parameter analysis of ERABiLNet.

Sl. No	Name of the dataset source	Symbol	Description
1)	Learning Rate	α	This is the measure of the number of attempts the model needs to update itself during the error when the weights are reassigned. It is a crucial parameter in model checking for the deep learning models
2)	Batch Size	$[\bar{b}]$	This is the enhancement of the training, by dividing the training data into several batches for optimizing the training process
3)	Number of the Hidden Units	H	A hidden layer is a layer that handles transformation of data and processing layers between the input and the output layer. These are essential for the enhancement of the training and development of the model
4)	Number of the Epochs	E	The number of Epochs indicates the number of cycles required to train the model efficiently. The validation error is the measure of the training efficiency. The epochs may be increased, if the validation error is more
5)	Number of the Layers	L	The number of layers increases the convolution of the model. The increase in the number of the middle layer increases the performance and efficiency of the model. A Three-layer model performs much better than a two layer model
6)	Momentum	β	Momentum is a byper parameter in deep learning model, that accelerates the Gradient Descent function with the fraction of the previous update of the model with the current update

Metrics/ Algorithm	ROA-ERABi-LNet [29]	EOO-ERABi-LNet [30]	GTBO-ERABi-LNet [31]	SRO-ERABi-LNet [25]	MSRO-ERABi-LNET
Dataset 1					
Precision	91.690	93.571	94.840	96.068	97.398
FPR	8.358	6.469	5.190	3.953	2.616
F1-Score	91.686	93.591	94.844	96.053	97.374
Specificity	91.642	93.531	94.810	96.047	97.384
Sensitivity	91.683	93.610	94.848	96.037	97.349
Accuracy	91.663	93.571	94.829	96.042	97.367
MCC	0.833	0.871	0.897	0.921	0.947
NPV	91.635	93.570	94.818	96.015	97.335
FDR	8.310	6.429	5.160	3.932	2.602
FNR	8.317	6.390	5.152	3.963	2.651
Dataset 2					
Precision	91.941	93.774	94.923	96.236	97.432
FPR	8.275	6.395	5.219	3.868	2.642
F1-Score	91.822	93.668	94.855	96.159	97.413
Specificity	91.725	93.605	94.781	96.132	97.358
Sensitivity	91.704	93.563	94.786	96.081	97.393
Accuracy	91.714	93.584	94.784	96.106	97.376
MCC	0.834	0.872	0.896	0.922	0.947
NPV	91.482	93.388	94.640	95.973	97.317
FDR	8.059	6.226	5.077	3.764	2.568
FNR	8.296	6.437	5.214	3.919	2.607

Table 5. Algorithmic comparison of the developed AD detection framework.
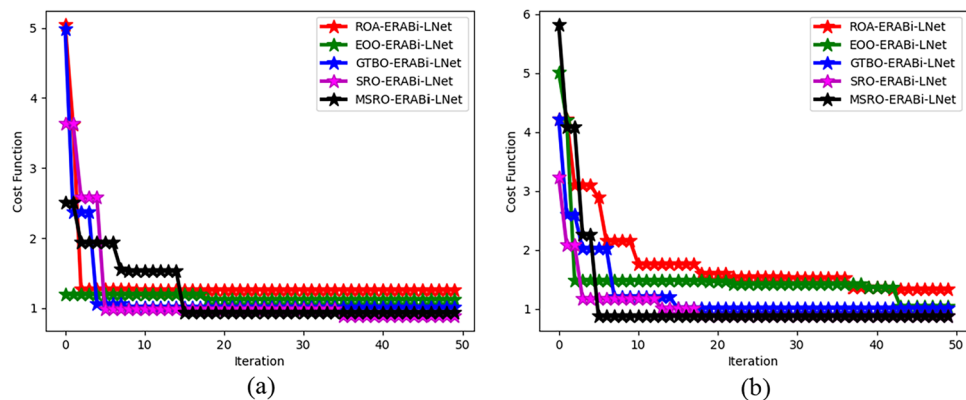

Fig. 15. Convergence Assessment of the Suggested AD Detection Model in terms of "(**a**) Dataset 1, and (**b**) Dataset 2".

Measures/ Algorithm	ROA-ERABi-LNet [29]	EOO-ERABi-LNet [30]	GTBO-ERABi-LNet [31]	SRO-ERABi-LNet [25]	MSRO-ERABi-LNET
Dataset 1					
Standard Deviation	0.618	0.034	0.632	0.637	0.436
Best	1.263	1.124	1.006	0.882	0.930
Median	1.263	1.124	1.006	0.989	0.930
Mean	1.386	1.150	1.174	1.158	1.190
Worst	5.039	1.195	4.978	3.634	2.503
Dataset 2					
Standard Deviation	0.671	0.654	0.581	0.400	0.948
Best	1.329	1.032	1.012	0.874	0.870
Median	1.534	1.415	1.012	0.874	0.870
Mean	1.802	1.511	1.251	1.042	1.153
Worst	4.223	5.012	4.219	3.229	5.816

Table 6. Statistical report on the implemented AD detection model.
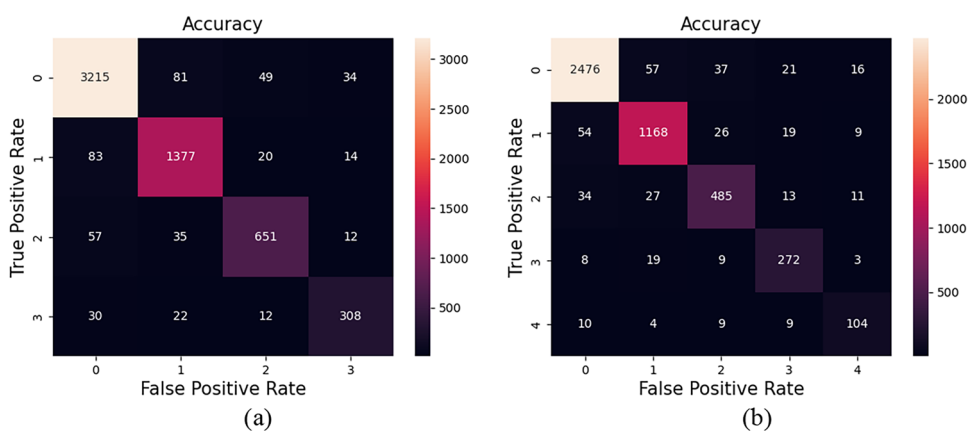

Fig. 16. Confusion Matrix Analysis of the Executed AD Detection Model regarding "(**a**) Dataset 1, and (**b**) Dataset 2.4

Data availability
The datasets used and/or analysed during the current study are available from the corresponding author on request.

References
1. Denis, A. *et al.* An effective deep residual network based class attention layer with bidirectional LSTM for diagnosis and classification of COVID-19. *J. Appl. Stat.* **50**, 477–494 (2020).
2. Sathish Kumar, L. *et al.* AlexNet approach for early stage Alzheimer's disease detection from MRI brain images. *Mater. Today Proc.* **51**, 58–65 (2022).
3. Yoon, H. *et al.* Automatic detection of amyloid beta plaques in somatosensory cortex of an Alzheimer's disease mouse using deep learning. *IEEE Access* **9**, 161926–161936 (2021).
4. Guo, H. & Zhang, Y. Resting state fMRI and improved deep learning algorithm for earlier detection of Alzheimer's disease. *IEEE Access* **8**, 115383–115392 (2020).
5. Subramanyam Rallabandi, V. P. & Seetharaman, K. Deep learning-based classification of healthy aging controls, mild cognitive impairment and Alzheimer's disease using fusion of MRI-PET imaging. *Biomed. Signal Process. Control* **80**, 104312 (2023).
6. Houria, L., Belkhamsa, N., Cherfa, A. & Cherfa, Y. Multi-modality MRI for Alzheimer's disease detection using deep learning. *Phys. Eng. Sci. Med.* **45**, 1043–1053 (2022).
7. Escudero, J. *et al.* Machine learning-based method for personalized and cost-effective detection of Alzheimer's disease. *IEEE Trans. Biomed. Eng.* **60**(1), 164–168 (2013).
8. Gamal, A., Elattar, M. & Selim, S. Automatic early diagnosis of Alzheimer's disease using 3D deep ensemble approach. *IEEE Access* **10**, 115974–115987 (2022).
9. Khan, Y. F., Kaushik, B., Rahmani, M. K. I. & Ahmed, M. E. Stacked deep dense neural network model to predict Alzheimer's dementia using audio transcript data. *IEEE Access* **10**, 32750–32765 (2022).
10. Chokri, R., Hanini, W., Daoud, W. B., Chelloug, S. A. & Makhlouf, A. M. Secure IoT assistant-based system for Alzheimer's disease. *IEEE Access* **10**, 44305–44314 (2022).

11. Han, R., Liu, Z. & Philip Chen, C. L. Multi-scale 3D convolution feature-based broad learning system for Alzheimer's disease diagnosis via MRI images. *Appl. Soft Comput.* **120**, 108660 (2022).
12. Ebrahimi, A., Luo, S. & Chiong, R. Deep sequence modelling for Alzheimer's disease detection using MRI. *Comput. Biol. Med.* **134**, 104537 (2021).
13. AtifMehmood, *et al.* A Transfer Learning Approach for Early Diagnosis of Alzheimer's Disease on MRI Images. *Neuroscience* **460**, 43–52 (2021).
14. Helaly, H. A., Badawy, M. & Haikal, A. Y. Deep learning approach for early detection of Alzheimer's disease. *Cognit. Comput.* **14**, 1711–1727 (2022).
15. Illakiya, T. & Karthik, R. Automatic detection of Alzheimer's disease using deep learning models and neuro-imaging: Current trends and future perspectives. *Neuroinformatics* **21**, 339–364 (2023).
16. Liu, S. *et al.* Generalizable deep learning model for early Alzheimer's disease detection from structural MRIs. *Sci. Rep.* **12**, 17106 (2022).
17. Taeho, J., Kwangsik, N., Risacher, S. L. & Saykin, A. J. Deep learning detection of informative features in tau PET for Alzheimer's disease classification. *BMC Bioinform.* **21**(1), 13 (2020).
18. MohanaRoopa, Y., Bhaskar Reddy, B., Babu, M. R. & Krishna Nayak, R. Teaching learning-based brain storm optimization tuned Deep-CNN for Alzheimer's disease classification. *Multimed. Tools Appl.* **82**, 33333–33356 (2023).
19. Subramanyam Rallabandi, V. P. & Seetharaman, K. Deep learning-based classification of healthy aging controls, mild cognitive impairment and Alzheimer's disease using fusion of MRI-PET imaging. *Biomed. Signal Process. Control* **80**, 104312. https://doi.org/10.1016/j.bspc.2022.104312 (2023).
20. Faisal, F. U. R. & Kwon, G.-R. Automated detection of Alzheimer's disease and mild cognitive impairment using whole brain MRI. *IEEE Access* **10**, 65055–65066 (2022).
21. Tanveer, M. *et al.* Classification of Alzheimer's disease using ensemble of deep neural networks trained through transfer learning. *IEEE J. Biomed. Health Inform.* **26**(4), 1453–1463 (2022).
22. Fareed, M. M. S., ShahidZikria, G. A., Mui-Zzud-Di, S. M. & Aslam, M. ADD-Net: An effective deep learning model for early detection of Alzheimer disease in MRI scans. *IEEE Access* **10**, 96930–96951 (2022).
23. Sharma, S., Guleria, K., Tiwari, S. & Kumar, S. A deep learning based convolutional neural network model with feature extractor for the detection of Alzheimer disease using MRI scans. *Meas. Sens.* **24**, 100506 (2022).
24. Liu, Y., Mazumdar, S. & Bath, P. A. An unsupervised learning approach to diagnosing Alzheimer's disease using brain magnetic resonance imaging scans. *Int. J. Med. Inform.* **173**, 105027 (2023).
25. Sharma, R., TriptiGoel, M. T. & Murugan, R. FDN-ADNet: Fuzzy LS-TWSVM based deep learning network for prognosis of the Alzheimer's disease using the sagittal plane of MRI scans. *Appl. Soft Comput.* **115**, 108099 (2022).
26. Rahul, K., Kumarb, R. & Banyalc,. Rider optimization algorithm (ROA): An optimization solution for engineering problem. *Turk. J. Comput. Math. Edu.* **12**(12), 3197–3201 (2021).
27. Borkar, P. *et al.* Deep learning and image processing-based early detection of Alzheimer disease in cognitively normal individuals. *Soft Comput.* 1–23. https://doi.org/10.1007/s00500-023-08615-w (2023).
28. Dua, M., Makhija, D., Manasa, P. Y. L. & Mishra, P. A CNN–RNN–LSTM based amalgamation for Alzheimer's disease detection. *J. Med. Biol. Eng.* **40**, 688–706 (2020).
29. Ramanathan, S. & Ramasundaram, M. Alzheimer's disease shape detection model in brain magnetic resonance images via whale optimization with kernel support vector machine. *J. Electr. Eng. Technol.* **18**, 2287–2296 (2023).
30. Cilia, N. D., D'Alessandro, T., De Stefano, C., Fontanella, F. & Molinara, M. From online handwriting to synthetic images for Alzheimer's disease detection using a deep transfer learning approach. *IEEE J. Biomed. Health Inform.* **25**(12), 4243–4254 (2021).
31. Ahmed, S. *et al.* Ensembles of patch-based classifiers for diagnosis of Alzheimer diseases. *IEEE Access* **7**, 73373–73383 (2019).
32. Chabib, C. M., Hadjileontiadis, L. J. & Shehhi, A. A. DeepCurvMRI: Deep convolutional curvelet transform-based MRI approach for early detection of Alzheimer's disease. *IEEE Access* **11**, 44650–44659 (2023).
33. Dao, Q., El-Yacoubi, M. A. & Rigaud, A.-S. Detection of Alzheimer disease on online handwriting using 1D convolutional neural network. *IEEE Access* **11**, 2148–2155 (2023).
34. Fabietti, M. *et al.* Early detection of Alzheimer's disease from cortical and hippocampal local field potentials using an ensembled machine learning model. *IEEE Trans. Neural Syst. Rehabilit. Eng.* **31**, 2839–2848 (2023).
35. Miltiadous, A., Gionanidis, E., Tzimourta, K. D., Giannakeas, N. & Tzallas, A. T. DICE-Net: A novel convolution-transformer architecture for Alzheimer detection in EEG signals. *IEEE Access* **11**, 71840–71858 (2023).
36. Ju, R., Hu, C. & p. zhou and Q. Li,. Early diagnosis of Alzheimer's disease based on resting-state brain networks and deep learning. *IEEE/ACM Trans. Comput. Biol. Bioinform.* **16**(1), 244–257 (2019).
37. Afzal, S. *et al.* A Data augmentation-based framework to handle class imbalance problem for Alzheimer's stage detection. *IEEE Access* **7**, 115528–115539 (2019).
38. Alvi, A. M., Siuly, S. & Wang, H. A long short-term memory based framework for early detection of mild cognitive impairment from EEG signals. *IEEE Trans. Emerg. Topics Comput. Intell.* **7**(2), 375–388 (2023).
39. Jiménez-Mesa, C. *et al.* Optimized one vs one approach in multiclass classification for early Alzheimer's disease and mild cognitive impairment diagnosis. *IEEE Access* **8**, 96981–96993 (2020).
40. Sekhar, B. V. D. S. & Jagadev, A. K. Efficient Alzheimer's disease detection using deep learning technique. *Soft Comput.* **27**, 9143–9150 (2023).
41. Raghavaiah, P. & Varadarajan, S. A CAD system design to diagnosize Alzheimers disease from MRI brain images using optimal deep neural network. *Multimed. Tools Appl. v* **80**, 26411–26428 (2021).
42. Mahendran, N. & Durai Raj Vincent, P. M. A deep learning framework with an embedded-based feature selection approach for the early detection of the Alzheimer's disease. *Comput. Biol. Med.* **141**, 105056 (2022).
43. Abuhmed, T., El-Sappagh, S. & Alonso, J. M. Robust hybrid deep learning models for Alzheimer's progression detection. *Knowl. Based Syst.* **213**, 106688 (2021).
44. El-Sappagh, S., Tamer Abuhmed, S. M., Islam, R. & Kwak, K. S. Multimodal multitask deep learning model for Alzheimer's disease progression detection based on time series data. *Neurocomputing* **412**, 197–215 (2020).
45. Alorf, A. & Khan, M. U. G. Multi-label classification of Alzheimer's disease stages from resting-state fMRI-based correlation connectivity data and deep learning. *Comput. Biol. Med.* **151**, 106240 (2022).
46. Orouskhani, M. *et al.* Alzheimer's disease detection from structural MRI using conditional deep triplet network. *Neurosci. Inform.* **2**(4), 100066. https://doi.org/10.1016/j.neuri.2022.100066 (2022).
47. de Silva, K. & Kunz, H. Prediction of Alzheimer's disease from magnetic resonance imaging using a convolutional neural network. *Intell. Based Med.* **7**, 100091. https://doi.org/10.1016/j.ibmed.2023.100091 (2023).
48. El-Assy, A. M., Amer, H. M., Ibrahim, H. M. & Mohamed, M. A. A novel CNN architecture for accurate early detection and classification of Alzheimer's disease using MRI data. *Sci. Rep.* **14**(1), 3463. https://doi.org/10.1038/s41598-024-53733-6 (2024).
49. Pradhan, N., Sagar, S. & Singh, A. Analysis of MRI image data for Alzheimer disease detection using deep learning techniques. *Multimed. Tools Appli.* **83**, 1–24. https://doi.org/10.1007/s11042-023-16256-2 (2023).
50. Nagarathna, C. R. & Kusuma, M. M. Early detection of Alzheimer's Disease using MRI images and deep learning techniques. *Alzheimer's Dement.* **19**(S3), e062076. https://doi.org/10.1002/alz.062076 (2023).

51. Chen, Y., Xia, R., Yang, K. & Zou, K. MICU: Image super-resolution via multi-level information compensation and U-net. *Expert Syst. Appli.* **245**, 123111 (2024).
52. Chen, Y., Xia, R., Yang, K. & Zou, K. MFMAM: Image inpainting via multi-scale feature module with attention module. *Comput. Vis. Image Underst.* **238**, 103883 (2024).
53. Chen, Y., Xia, R., Yang, K. & Zou, K. GCAM: Lightweight image inpainting via group convolution and attention mechanism. *Int. J. Mach. Learn. Cybern.* **15**. https://doi.org/10.1007/s13042-023-01999-z (2023).
54. Chen, Y., Xia, R., Yang, K. & Zou, K. DNNAM: Image inpainting algorithm via deep neural networks and attention mechanism. *Appl. Soft Comput.* **154**, 111392. https://doi.org/10.1016/j.asoc.2024.111392 (2024).
55. Singh, S. *et al.* Efficient pneumonia detection using vision transformers on chest X-rays. *Sci. Rep.* **14**, 2487. https://doi.org/10.1038/s41598-024-52703-2 (2024).
56. M. Frey, C. F. Doeller and C. Barry, "Probing Neural Representations of Scene Perception in a Hippocampally Dependent Task Using Artificial Neural Networks," 2023 IEEE/CVF Conference on Computer Vision and Pattern Recognition (CVPR), Vancouver, BC, Canada, 2023, pp. 2113–2121, https://doi.org/10.1109/CVPR52729.2023.00210
57. Li, G., Zhao, L., Sun, J., Lan, Z., Zhang, Z., Chen, J., ... & Xing, W. (2023). Rethinking multi-contrast mri super-resolution: Rectangle-window cross-attention transformer and arbitrary-scale upsampling. In Proceedings of the IEEE/CVF International Conference on Computer Vision (pp. 21230–21240).
58. Lamb, N., Banerjee, S., & Banerjee, N. K. (2022, October). Deepmend: Learning occupancy functions to represent shape for repair. In European Conference on Computer Vision (pp. 433–450). Cham: Springer Nature Switzerland.
59. Shabani, A., Asgarian, B., AsilGharebaghi, S., Salido, M. A. & Giret, A. A new optimization algorithm based on search and rescue operations. *Math. Probl. Eng.* **2482543**, 23 (2019).
60. Omid Tarkhaneh, Neda Alipour, Amirahmad Chapnevis, and Haifeng Shen, "Golden Tortoise Beetle Optimizer: A Novel Nature-Inspired Meta-heuristic Algorithm for Engineering Problems," Neural and Evolutionary Computing, 4 April 2021.
61. Shu, X., Zhang, L., Sun, Y. & Tang, J. Host–parasite: Graph LSTM-in-LSTM for group activity recognition. *IEEE Trans. Neural Netw. Learn. Syst.* **32**(2), 663–674 (2021).
62. Salim, A., Jummar, W. K., Jasim, F. M. & Yousif, M. Eurasian oystercatcher optimiser: New meta-heuristic algorithm. *J. Intell. Inf. Syst.* **31**, 332–344. https://doi.org/10.1515/jisys-2022-0017 (2022).
63. Ye, H. *et al.* Web services classification based on wide & Bi-LSTM model. *IEEE Access* **7**, 43697–43706 (2019).
64. Ramasamy, J., Ravikumar, R. N. & Shitharth, S. Artificial Neural Networks for Data Processing. In *A Case Study of Image Classification Advances Mathematical Applications in Data Science* (eds Malik, B. B. *et al.*) (Bentham Books, UK, 2023).
65. Ebrahimi, A. & Luo, S. Alzheimer's disease neuroimaging initiative convolutional neural networks for Alzheimer's disease detection on MRI images. *J. Med. Imaging (Bellingham)* **8**(2), 024503. https://doi.org/10.1117/1.JMI.8.2.024503 (2021).
66. Eke, C. S. *et al.* Early detection of Alzheimer's disease with blood plasma proteins using support vector machines. *IEEE J. Biomed. Health Inform.* **25**, 218–226 (2021).
67. Ahmed, S. *et al.* Att-BiL-SL: Attention-based Bi-LSTM and sequential LSTM for describing video in the textual formation. *Appl. Sci.* **12**(1), 317 (2022).
68. Helaly, H. A., Badawy, M. & Haikal, A. Y. Deep learning approach for early detection of Alzheimer's disease. *Cogn. Comput.* **14**, 1711–1727. https://doi.org/10.1007/s12559-021-09946-2 (2022).
69. Leonardis, A., Bischof, H., & Pinz, A. (Eds.) (2006). Computer Vision - ECCV 2006, 9th European Conference on Computer Vision, Proceedings, Part I. Springer.
70. Fareed, *et al.* ADD-Net: An Effective Deep Learning Model for Early Detection of Alzheimer Disease in MRI Scans. *IEEE Access* https://doi.org/10.1109/ACCESS.2022.3204395 (2022).
71. Shankar, N., Nallakaruppan, M. K., Ravindranath, V., Senthilkumar, M. & Bhagavath, B. P. Smart IoMT framework for supporting UAV systems with AI. *Electronics* **12**(1), 86. https://doi.org/10.3390/electronics12010086 (2023).
72. Dass, R. *et al.* A cluster-based energy-efficient secure optimal path-routing protocol for wireless body-area sensor networks. *Sensors* **23**(14), 6274. https://doi.org/10.3390/s23146274 (2023).
73. Dhingra, N. & Kunz, A. Res3ATN – deep 3D residual attention network for hand gesture recognition in videos. *Comput. Vis. Pattern Recognit.* **4**, 491–501 (2020).
74. Ma, Z., Zhang, H. & Liu, J. MM-RNN: A multimodal RNN for precipitation nowcasting. *IEEE Trans. Geosci. Remote Sens.* **61**, 1–14 (2023).
75. Nallakaruppan, M. K. *et al.* Reliable water quality prediction and parametric analysis using explainable AI models. *Sci. Rep.* **14**, 7520. https://doi.org/10.1038/s41598-024-56775-y (2024).

Author contributions

All authors contributed equally to this work. All authors reviewed the manuscript.

Competing interests

The authors declare no competing interests.

Additional information

Correspondence and requests for materials should be addressed to S.S.

Reprints and permissions information is available at www.nature.com/reprints.

Publisher's note Springer Nature remains neutral with regard to jurisdictional claims in published maps and institutional affiliations.